



HAL
open science

Reduced Order Models for a LNT-SCR Diesel After-treatment Architecture with NO/NO₂ Differentiation

David Marie-Luce, Pierre-Alexandre Bliman, Di-Penta Damiano, Michel
Sorine

► **To cite this version:**

David Marie-Luce, Pierre-Alexandre Bliman, Di-Penta Damiano, Michel Sorine. Reduced Order Models for a LNT-SCR Diesel After-treatment Architecture with NO/NO₂ Differentiation. [Research Report] RR-7913, INRIA. 2012, pp.46. hal-00682731

HAL Id: hal-00682731

<https://inria.hal.science/hal-00682731>

Submitted on 26 Mar 2012

HAL is a multi-disciplinary open access archive for the deposit and dissemination of scientific research documents, whether they are published or not. The documents may come from teaching and research institutions in France or abroad, or from public or private research centers.

L'archive ouverte pluridisciplinaire **HAL**, est destinée au dépôt et à la diffusion de documents scientifiques de niveau recherche, publiés ou non, émanant des établissements d'enseignement et de recherche français ou étrangers, des laboratoires publics ou privés.



Reduced Order Models for a LNT-SCR Diesel After-treatment Architecture with NO/NO₂ Differentiation

David Marie-Luce, Pierre-Alexandre Bliman, Damiano Di-Penta,
Michel Sorine

**RESEARCH
REPORT**

N° 7913

March 2012

Project-Team SISYPHE



Reduced Order Models for a LNT-SCR Diesel After-treatment Architecture with NO/NO₂ Differentiation

David Marie-Luce*, Pierre-Alexandre Bliman[†], Damiano
Di-Penta*, Michel Sorine[†]

Project-Team SISYPHE

Research Report n° 7913 — March 2012 — 43 pages

Abstract: LNT and SCR are two leading candidates for Diesel exhaust nitrogen oxide (NO_x) after-treatment. The present paper investigates the modeling of the architecture combining the two systems in series with NO/NO₂ differentiation, induced directly by the widening and hardening of the future standards. Model reduction is performed to allow for real-time automotive applications. Based on simplified chemistry and slow-fast dynamics assumptions, a complete reduced model is proposed, suitable for on-board diagnosis and model-based control. Validation has been achieved through extensive experiments.

Key-words: After-treatment system modeling, nonlinear system, Model reduction, validation

* Technocentre Renault Guyancourt, 1 avenue du golf, 78288 Guyancourt, France

[†] INRIA Rocquencourt, Domaine de Voluceau, 78153 Le Chesnay cedex, France

**RESEARCH CENTRE
PARIS – ROCQUENCOURT**

Domaine de Voluceau, - Rocquencourt
B.P. 105 - 78153 Le Chesnay Cedex

Modélisation réduite d'éléments d'une architecture de post-traitement Diesel LNT-SCR avec différenciation NO/NO₂

Résumé : Les, Piège à NO_x et SCR sont deux systèmes catalytiques à fort potentiel de réduction des émissions d'oxydes d'azote. Le document décrit la modélisation de ces éléments de post-traitement des gaz d'échappement, dans le cadre de l'étude d'une architecture combinant les deux systèmes mis en série. La particularité de ce travail repose sur la différenciation NO/NO₂ dans la modélisation, induite par l'apparition de nouvelles normes plus sévères et couvrant plus d'espèces chimiques. Une réduction d'ordre des modèles basée sur la séparation des échelles de temps est ensuite appliquée en vue du respect des contraintes de calcul en temps réel émanant de l'industrie automobile. Ainsi, à partir de ces hypothèses et après proposition d'un schéma cinétique simplifié, un modèle d'ordre réduit adapté à l'élaboration de stratégies de contrôle est proposé et validé avec des essais expérimentaux.

Mots-clés : Modélisation, Post-traitement Diesel, Système non-linéaire, Réduction de modèles, Validation

Contents

1	Introduction	5
2	State of the art on chemical modeling of LNT and SCR	6
2.1	Operation of a NO _x Trap	6
2.1.1	Storage	7
2.1.2	Regeneration	8
2.2	Operation of a SCR	8
2.2.1	Ammonia storage	9
2.2.2	Selective reduction principle, [18, 20]	9
3	Chemical model reduction by species aggregation	9
3.1	SCR chemical reduction	10
4	Kinetic modeling	11
4.1	Assumptions	11
4.2	LNT Kinetic model	12
4.3	SCR kinetic model	12
5	Reduction by Singular perturbation	12
5.1	Assumptions	13
5.2	LNT model	13
5.3	SCR model	14
6	Properties of the reduced models	15
6.1	Assumption	15
6.2	Resolution of the algebraic equations and stability issues	16
6.2.1	LNT reduced order model	16
6.2.2	SCR reduced order model	22
6.3	Global reduced system	24
6.4	Boundedness of the coverage fractions	25
6.5	Further reduction of the models	26
6.5.1	Assumptions	26
6.5.2	Resulting model	27
7	Experimental results	29
7.1	Lean NO _x Trap catalyst	29
7.1.1	Method	29
7.1.2	Results	30
7.2	SCR catalyst : Calibration	32
7.2.1	Method	32
7.2.2	Results	33
7.3	SCR catalyst : Validation	34
8	Summary/Conclusions	36

A	Definitions/Abbreviations	37
A.1	Indexes/exponents	37
A.2	Greek/Latin letters	37
B	Proof of (45)	38

1 Introduction

This paper focus on the control-oriented modeling of a future after-treatment line for Euro 6 or even Euro 7 vehicles. These forthcoming standards lay down stricter boundaries on pollutant emissions and new restricted species notably NO and NO₂. The European manufacturers have thus to integrate the presence of these new species in the modeling of each catalytic feature of the exhaust line.

The automotive industry increasingly uses models, allowing for lower costs and more flexible processes as simulation can replace real driving tests. The models studied in the present paper are aimed at control and diagnosis applications, this is the reason why model complexity reduction is emphasized.

A large number of articles on chemical principles and experimental studies of hybrid catalytic systems composed of Lean NO_x Trap (LNT) and Selective Catalytic Reduction catalyst (SCR) have appeared recently, see e.g. [1], [2], [3], [4]. Fewer are devoted to modeling and in general, too complex for control applications. Moreover, the available models are indeed incomplete and unable to cope with the new norms, due to the new species of restricted pollutants that have to be incorporated.

This work follows the one described in [5] in which a simplified model of the architecture combining a LNT followed by a SCR is concerned regarding NO_x reduction with ammonia production ([6], [7], [8]). The models are improved here by introducing NO and NO₂ contribution from engine running. Formation of ammonia during the rich phases of the LNT functioning is also considered.

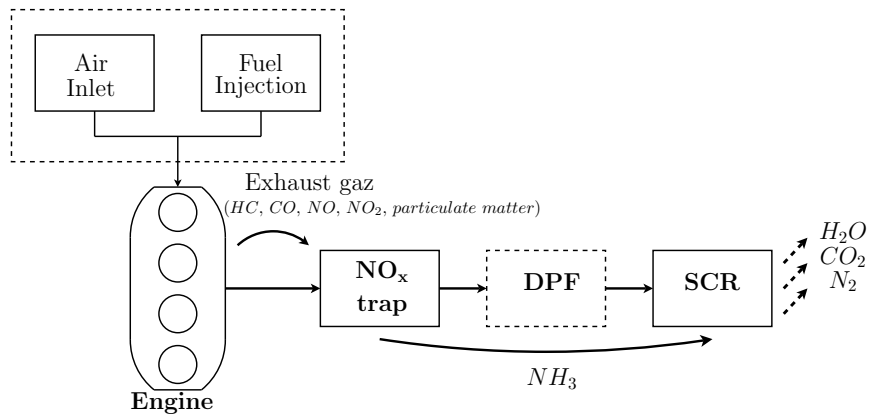


Figure 1: Principle of a combined exhaust after-treatment system consisting of NO_x storage reduction catalyst(LNT) and selective catalytic reduction of NO_x by NH₃ (SCR)

The paper describes, in a first part, a NO_x after-treatment system for diesel engines (Figure 1) including (from upstream to downstream): a lean NO_x trap, a Diesel Particulate Filter (DPF) to treat the particulate matter, and a SCR catalyst. In our modeling, one considers the architecture composed of the LNT and SCR in series ⁽¹⁾, according to Figure 2.

⁽¹⁾For our purpose one neglects the passive regeneration of the DPF (see [9], [10]).

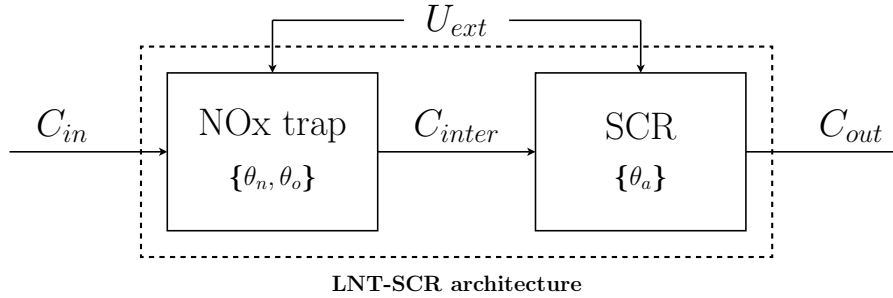


Figure 2: Scheme of the studied architecture. The subscripts "in", "inter" and "out" refers respectively to the LNT catalyst input, the LNT output/SCR input and the SCR output; U_{ext} corresponds to the exogenous inputs, namely the inlet gas temperature and the exhaust speed

NO_x reduction in LNT is operated cyclically. In normal (lean) mode, Diesel engine exhaust NO_x is stored on the catalyst. Then when necessary, by active control of the engine operating point, the composition of the exhaust gas is changed in order to treat the stored NO_x . This operating mode has the benefit of using on-board fuel as NO_x reducer. However NO_x trap solution is restrained by limited active temperature windows.

NH_3 -SCR catalysts operate in a wider range of temperature and do not contain precious metals. NH_3 -SCR systems traditionally use urea-water solution as reducing agent, requiring thus additional infrastructure to supply the vehicles with enough reducer. The NH_3 resulting from the urea solution hydrolysis is stored into the catalyst, allowing to reduce continuously the NO_x contained in the exhaust gas within three main reactions discussed in Section 2.

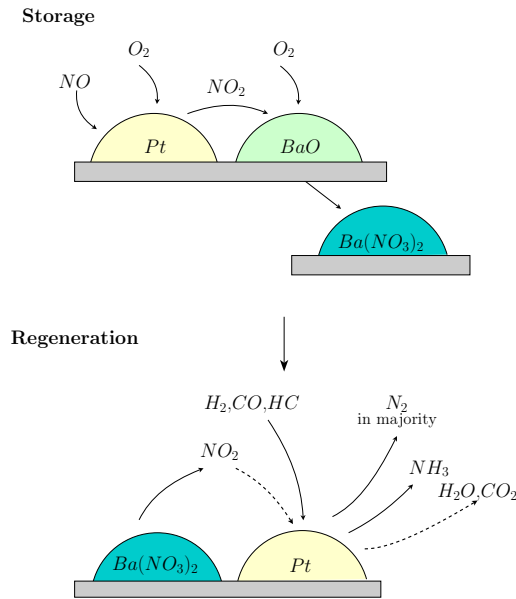
The pros and cons previously described are quite restrictive in classical LNT or NH_3 -SCR architecture. It turns out that synergy of the two systems is possible if the SCR takes advantage of the LNT ability to produce Ammonia (NH_3). Indeed, during the rich phases (purges), small amounts of Ammonia are formed as by-product, which can be used in the downstream catalyst as the NO_x reducing agent. Thus, an interesting issue is to analyse whether LNT-SCR architecture may improve the performance over traditional LNT systems, through adequate NO_x and NH_3 control : indeed this strategy would permit to reduce both NO_x and NH_3 at the same time. Furthermore, potential cost reduction can be obtained by elimination of the on-board urea storage and delivery system or size reduction of the LNT which contains precious metals.

In Section 2 a review on LNT and SCR modeling is presented. Section 3 presents a simplified version of the chemical schemes previously developed. Kinetic modeling of the reactions is described in Section 4. Then focus is put on model reduction for the whole system (see Section 5). Finally, the main model proposed herein is introduced with some properties (see Section 6). In a last stage, Section 7 presents results of calibration and validation through standard driving cycles.

2 State of the art on chemical modeling of LNT and SCR

2.1 Operation of a NO_x Trap

The mechanisms under consideration are summarized in Figure 3.

Figure 3: Operation of a NO_x trap

NO_x trap is operated in two operation conditions, namely *storage* (lean period) and *regeneration* (rich period). Many studies have been completed to identify and model mechanisms and kinetics of NO_x trap catalysts during both lean and rich operation, see [6], [7], [8], [11], [12], [13], [14] which are presented in the sequel.

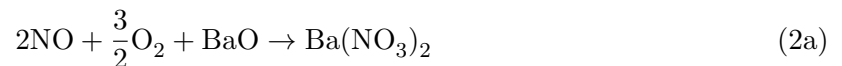
2.1.1 Storage

During the lean (or loading) mode, NO_x is stored on the catalyst in form of nitrate through a two-step process. First, NO is oxidized on Pt sites to form NO₂ and then adsorbed on metal (Barium) oxide sites. The mechanism is described by the following reactions.

Oxidation of NO to NO₂ [6], [13]



NO and NO₂ storage during lean mode [6],[8]



Addition of Cerium Oxides on the catalyst gives the ability to store Oxygen along the following reaction [15], [16].

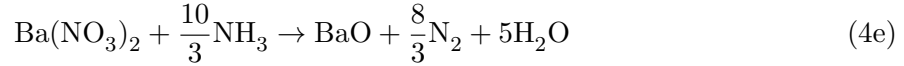
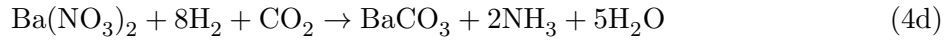
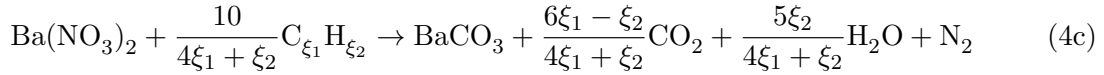
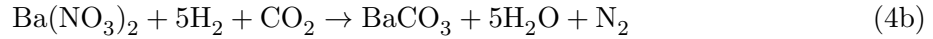
Oxygen storage



2.1.2 Regeneration

During the rich (or regeneration) mode, the Air Fuel Ratio (AFR) is increased in order to achieve reducing conditions. This is done by introduction of hydrocarbons in excess, which induce degradation of the combustion and release of reducing species under the form HC, CO and H₂. During these purge phases the stored NO_x and Oxygen are treated by the reducing species according to the following reactions.

Decomposition of the stored NO_x during rich time with the reducers, [6]-[8], [14]



Oxygen reduction



During the purges, high temperatures result in the release of some SO₂ but also large quantities of H₂S. Although the latter is not a regulated pollutant, it is a source of consumer dissatisfaction and should be drastically reduced. This requires an additional catalyst that is not considered in this work.

2.2 Operation of a SCR

The mechanisms under consideration are summarized in Figure 4.

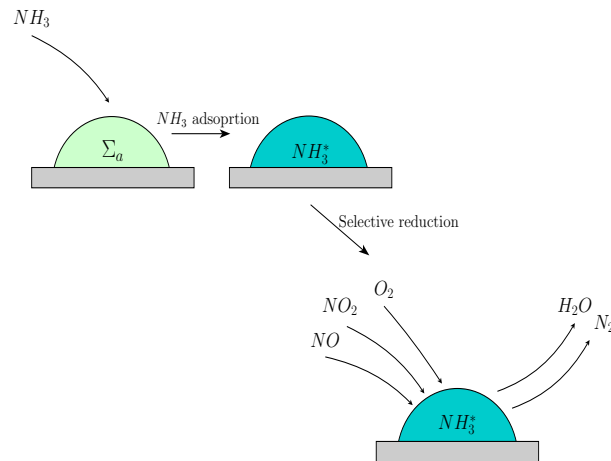


Figure 4: Operation of a SCR

SCR converter directly reduces NO_x emissions to non-pollutant species with the help of ammonia. This technology demonstrates good selectivity to NO_x and a great potential for

exhaust gas cleaning through the so-called *Selective Catalytic Reduction* process. In classical NH_3 -SCR architecture the formation of NH_3 arises from urea hydrolysis [17]. In our case, ammonia comes from the purges of the upstream catalyst.

Models for SCR catalysts include an NH_3 storage process occurring on the catalytic sites (denoted Σ_a in the sequel) usually composed of V_2O_5 , Ti_2O and WO_3 . The stored Ammonia then reacts selectively with NO_x in the presence of Oxygen, releasing nitrogen and vapor according to reactions which are now presented (see [17], [18], [19], [20] for details).

2.2.1 Ammonia storage

Adsorption and desorption of ammonia are described in (6), and (7) presents the ammonia oxidation, an undesired reaction which occurs at high temperature (above 400°C) with a selective formation of Nitrogen, [18], [20].

Adsorption/desorption process

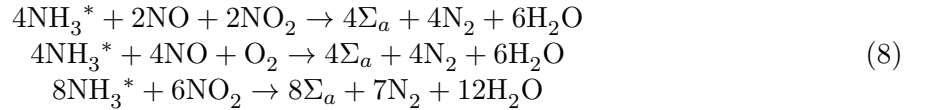


Oxidation process



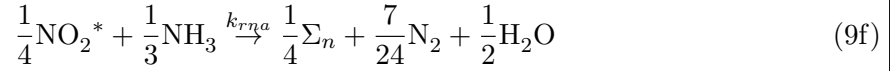
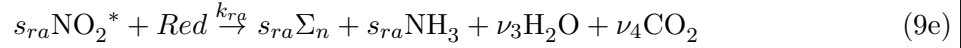
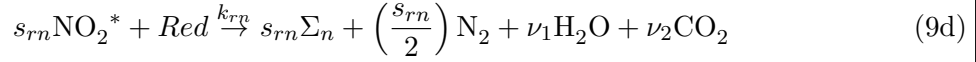
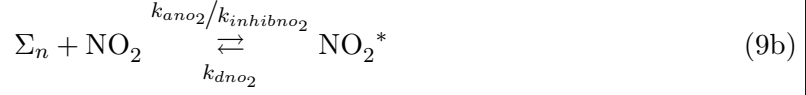
2.2.2 Selective reduction principle, [18, 20]

Selective Reduction is mainly based on three reactions respectively named *Fast SCR reaction*, *Standard SCR reaction* and *NO_2 -SCR reaction*. The so-called Fast SCR reaction describes the fast reaction taking place when NO and NO_2 are both present in the feed gas. According to the Standard SCR reaction equimolar amounts of NO and NH_3 react with Oxygen, to form Nitrogen and water. Then in the NO_2 -SCR reaction, NH_3 and NO_2 also react alone to form the same products.



3 Chemical model reduction by species aggregation

A simplified chemical scheme of reactions representing NO , NO_2 and Oxygen storage and reduction with ammonia production in the NO_x trap is considered. A main feature of the reduction achieved here is the introduction of a unique fictitious reducing species *Red* referring to HC , CO and H_2 . Based on the model developed in section 2.1, this new scheme results from the aggregation of (1), (2a), (2a) as the storage process (9a)-(9c), the aggregation of (4a)-(4f) as the regeneration process with ammonia production (9d)-(9f) and the substitution of (3) and (5) by (9g) and (9h).



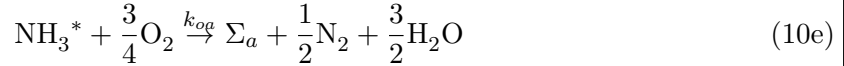
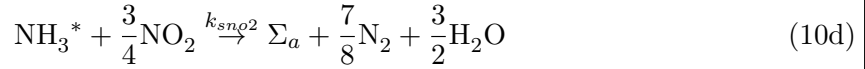
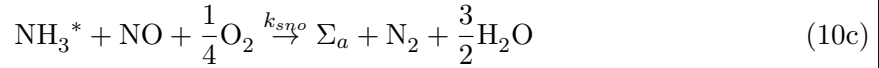
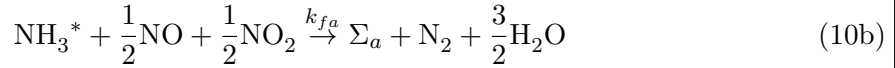
Here :

- Σ_n, Σ_o denote respectively free NO_2 and O_2 adsorption sites,
- $\text{NO}_2^*, \text{O}^*$ denote respectively occupied NO_2 and O_2 adsorption sites,
- The constants s, ν are positive integers which denote stoichiometric coefficients.

The symbols k put on top and bottom of the arrows are kinetic coefficients, see details below in section 4 and Appendix A.

3.1 SCR chemical reduction

The SCR model is kept unchanged :



4 Kinetic modeling

4.1 Assumptions

- Each subsystem is considered as a CSTR (Continuous Stirred Tank Reactor) with homogeneous mixing at homogeneous temperature. The temperatures are measured.
- The rates of reaction are expressed following kinetic laws of the type:

$$r_i = k_i \prod_j C_j^{\beta_{i,j}} \quad (11)$$

The $\beta_{i,j}$ are reaction orders, whose values will be determined through identification or fixed according to the existing literature. It is important however to state that they are positive real numbers. It is assumed that the kinetic coefficients k_i follow Arrhenius law :

$$k_i = k_i^0 \exp\left(-\frac{E_i}{RT}\right) \quad (12)$$

where k_i^0, E, R, T are respectively the pre-exponential constant, the activation energy, the gas constant and the catalyst temperature. The list of indexes introduced in (11) and (12) is defined in Appendix A.

The rates of reaction are now detailed, for the LNT:

$$r_{oxno} = k_{oxno} C_{no}^{inter} \quad (13a)$$

$$r_{rno_2} = k_{rno_2} C_{no_2}^{inter} \quad (13b)$$

$$r_{ano} = k_{ano} (\rho_n (1 - \theta_n))^{\beta_{ano}} C_{no}^{inter} \quad (13c)$$

$$r_{ano_2} = \frac{k_{ano_2} (\rho_n (1 - \theta_n))^{\beta_{ano_2}}}{1 + k_{inhibno_2} \theta_n} C_{no_2}^{inter} \quad (13d)$$

$$r_{dno_2} = k_{dno_2} (\rho_n \theta_n)^{\beta_{dno_2}} \quad (13e)$$

$$r_{ao} = k_{ao} (\rho_o (1 - \theta_o))^{\beta_{ao}} C_o^{inter} \quad (13f)$$

$$r_{rn} = k_{rn} (\rho_n \theta_n)^{\beta_{rn}} C_{red}^{inter} \quad (13g)$$

$$r_{ra} = k_{ra} (\rho_n \theta_n)^{\beta_{ra}} C_{red}^{inter} \quad (13h)$$

$$r_{rna} = k_{rna} (\rho_n \theta_n)^{\beta_{rna}} C_a^{inter} \quad (13i)$$

$$r_{rao} = k_{rao} (\rho_o \theta_o)^{\beta_{rao}} C_{red}^{inter} \quad (13j)$$

and for the SCR :

$$r_{aa} = k_{aa} (\rho_a (1 - \theta_a))^{\beta_{aa}} C_a^{out} \quad (14a)$$

$$r_{da} = k_{da} (\rho_a \theta_a)^{\beta_{da}} \quad (14b)$$

$$r_{oa} = k_{oa} (\rho_a \theta_a)^{\beta_{oa}} \quad (14c)$$

$$r_{sno} = k_{sno} (\rho_a \theta_a)^{\beta_{sno}} C_{no}^{out} \quad (14d)$$

$$r_{sno_2} = k_{sno_2} (\rho_a \theta_a)^{\beta_{sno_2}} C_{no_2}^{out} \quad (14e)$$

$$r_{fa} = k_{fa} (\rho_a \theta_a)^{\beta_{fa}} C_{no}^{out} C_{no_2}^{out} \quad (14f)$$

where ρ_n, ρ_o, ρ_a denote the density of sites on the catalyst layer, respectively, for NO_x , O_2 and NH_3 .

We will use the following notations in the writing of the conservation equations :

- v_{ech}^n, v_{ech}^s exhaust gas speed, respectively, in the LNT and the SCR,
- $\mathcal{L}_{pn}, \mathcal{L}_{scr}$ Characteristic length, respectively, of the LNT and the SCR,

4.2 LNT Kinetic model

Using the conservation equations, one may write the rate of change of each species in the NO_x trap. The following equations are considered :

$$\frac{dC_{no}^{inter}}{dt} = \frac{v_{ech}^n}{\mathcal{L}_{pn}}(C_{no}^{in} - C_{no}^{inter}) - r_{oxno} + r_{rno2} - r_{ano} \quad (15a)$$

$$\frac{dC_{no2}^{inter}}{dt} = \frac{v_{ech}^n}{\mathcal{L}_{pn}}(C_{no2}^{in} - C_{no2}^{inter}) + r_{oxno} - r_{rno2} - r_{ano2} + r_{dno2} \quad (15b)$$

$$\frac{dC_o^{inter}}{dt} = \frac{v_{ech}^n}{\mathcal{L}_{pn}}(C_o^{in} - C_o^{inter}) - r_{ao} \quad (15c)$$

$$\frac{dC_{red}^{inter}}{dt} = \frac{v_{ech}^n}{\mathcal{L}_{pn}}(C_{red}^{in} - C_{red}^{inter}) - r_{rn} - r_{ra} - r_{rao} \quad (15d)$$

$$\frac{dC_a^{inter}}{dt} = \frac{v_{ech}^n}{\mathcal{L}_{pn}}(C_a^{in} - C_a^{inter}) + s_{ra}r_{ra} - \frac{r_{rna}}{3} \quad (15e)$$

$$\rho_n \frac{d\theta_n}{dt} = r_{ano2} - r_{dno2} + r_{ano} - s_{rn}r_{rn} - s_{ra}r_{ra} - \frac{r_{rna}}{4} \quad (15f)$$

$$\rho_o \frac{d\theta_o}{dt} = r_{ao} - r_{rao} \quad (15g)$$

4.3 SCR kinetic model

Using the conservation equations, one may write the rate of change of each species in the SCR. The following equations are considered :

$$\frac{dC_{no}^{out}}{dt} = \frac{v_{ech}^s}{\mathcal{L}_{scr}}(C_{no}^{inter} - C_{no}^{out}) - r_{sno} - \frac{r_{fa}}{2} \quad (16a)$$

$$\frac{dC_{no2}^{out}}{dt} = \frac{v_{ech}^s}{\mathcal{L}_{scr}}(C_{no2}^{inter} - C_{no2}^{out}) - r_{sno2} - \frac{r_{fa}}{2} \quad (16b)$$

$$\frac{dC_a^{out}}{dt} = \frac{v_{ech}^s}{\mathcal{L}_{scr}}(C_a^{in} - C_a^{out}) - r_{aa} + r_{da} \quad (16c)$$

$$\rho_a \frac{d\theta_a}{dt} = r_{aa} - r_{da} - r_{oa} - \frac{4}{3}r_{sno2} - r_{sno} - r_{fa} \quad (16d)$$

5 Reduction by Singular perturbation

The models concerned by this study are aimed at control and diagnosis applications. We now reduce their complexity in order to decrease the computational burden without affecting their accuracy. Equations (15) and (16) are suitable for classical reduction methods application,

notably time-scale separation of slow and fast dynamics. These methods consist in classifying the state variables according to their dynamics, considering that the fastest ones are perpetually at their equilibrium values driven by slow state variables. The new differential-algebraic system appears as a singular perturbation of the original one, retaining only the slow state variables. See [21].

5.1 Assumptions

On the one hand, in chemical engineering, it is often assumed that the evolution of gas phase species are infinitely fast, in the sense that the evolution of the whole gaz-phase (NO_x , reductant and product concentrations) is quasi-static. This assumption is called *non-accumulation of gaseous species* and leads to the singular perturbation situation.

On the other hand, Ceria is a key component for the treatment of the exhaust emission, as it acts as an oxygen buffer, releasing oxygen for CO and hydrocarbons in rich environment and storing oxygen from O_2 and NO in lean environment. Its ability to react fast with oxygen [16] makes the state parameter θ_o dynamically faster than θ_n and θ_a .

We will use the following exponents in the sequel :

- u , for the "upstream" catalyst (LNT),
- d , for the "downstream" catalyst (SCR),

5.2 LNT model

Under the assumptions stated in section 5.1, using equations (15), the LNT dynamic system is expressed by the following singularly perturbed system :

$$\varepsilon \frac{d\mathbf{C}^{\text{inter,u}}}{dt} = \frac{v_{ech}^n}{\mathcal{L}_{pn}} (\mathbf{C}^{\text{in}} - \mathbf{C}^{\text{inter,u}}) + \mathbf{K}_c^u (\mathbf{R}^u(\Theta)\mathbf{C}^{\text{inter,u}} + \bar{\mathbf{R}}^u(\Theta)) \quad (17a)$$

$$\begin{pmatrix} 1 & 0 \\ 0 & \varepsilon \end{pmatrix} \frac{d\Theta}{dt} = \mathbf{K}_\theta^u (\mathbf{R}^u(\Theta)\mathbf{C}^{\text{inter,u}} + \bar{\mathbf{R}}^u(\Theta)) \quad (17b)$$

with ε representing the perturbation scalar parameter, and where :

$$\mathbf{C}^{\text{in}} = \begin{pmatrix} C_{no}^{\text{in}} \\ C_{no_2}^{\text{in}} \\ C_o^{\text{in}} \\ C_{red}^{\text{in}} \\ C_a^{\text{in}} \end{pmatrix}, \quad \mathbf{C}^{\text{inter,u}} = \begin{pmatrix} C_{no}^{\text{inter}} \\ C_{no_2}^{\text{inter}} \\ C_o^{\text{inter}} \\ C_{red}^{\text{inter}} \\ C_a^{\text{inter}} \end{pmatrix}, \quad \Theta = \begin{pmatrix} \theta_n \\ \theta_o \end{pmatrix}, \quad (17c)$$

$$\mathbf{K}_c^u = \begin{pmatrix} -1 & 1 & -1 & 0 & 0 & 0 & 0 & 0 & 0 & 0 & 0 \\ 1 & -1 & 0 & -1 & 1 & 0 & 0 & 0 & 0 & 0 & 0 \\ 0 & 0 & 0 & 0 & 0 & -1 & 0 & 0 & 0 & 0 & 0 \\ 0 & 0 & 0 & 0 & 0 & 0 & -1 & -1 & 0 & 0 & -1 \\ 0 & 0 & 0 & 0 & 0 & 0 & 0 & 0 & s_{ra} & -\frac{1}{3} & 0 \end{pmatrix}, \quad (18)$$

$$\mathbf{K}_\theta^u = \begin{pmatrix} 0 & 0 & \frac{1}{\rho_n} & \frac{1}{\rho_n} & 0 & 0 & -\frac{s_{rn}}{\rho_n} & -\frac{s_{ra}}{\rho_n} & -\frac{1}{4\rho_n} & 0 \\ 0 & 0 & 0 & 0 & 0 & \frac{1}{\rho_o} & 0 & 0 & 0 & -\frac{1}{\rho_o} \end{pmatrix}, \quad (19)$$

$$\mathbf{R}^u(\Theta) = \begin{pmatrix} k_{oxno} & 0 & 0 & 0 & 0 \\ 0 & k_{rno2} & 0 & 0 & 0 \\ k_{ano}(\rho_n(1-\theta_n))^{\beta_{ano}} & 0 & 0 & 0 & 0 \\ 0 & \frac{k_{ano2}(\rho_n(1-\theta_n))^{\beta_{ano2}}}{1+k_{inhibno2}\theta_n} & 0 & 0 & 0 \\ 0 & 0 & 0 & 0 & 0 \\ 0 & 0 & k_{ao}(\rho_o(1-\theta_o))^{\beta_{ao}} & 0 & 0 \\ 0 & 0 & 0 & 0 & 0 \\ 0 & 0 & 0 & k_{rn}(\rho_n\theta_n)^{\beta_{rn}} & 0 \\ 0 & 0 & 0 & k_{ra}(\rho_n\theta_n)^{\beta_{ra}} & 0 \\ 0 & 0 & 0 & 0 & k_{rna}(\rho_n\theta_n)^{\beta_{rna}} \\ 0 & 0 & 0 & k_{rao}(\rho_o\theta_o)^{\beta_{rao}} & 0 \end{pmatrix}, \quad (20)$$

$$\bar{\mathbf{R}}^u(\Theta) = \begin{pmatrix} 0 \\ 0 \\ 0 \\ 0 \\ k_{dno2}(\rho_n\theta_n)^{\beta_{dno2}} \\ 0 \\ 0 \\ 0 \\ 0 \\ 0 \end{pmatrix}. \quad (21)$$

5.3 SCR model

Under the assumptions stated in section 5.1, using equations (16), the SCR dynamic system is expressed by the following singularly perturbed system :

$$\varepsilon \frac{d\mathbf{C}^{\text{out}}}{dt} = \frac{v_{ech}^s}{\mathcal{L}_{scr}} \left(\mathbf{C}^{\text{inter,d}} - \mathbf{C}^{\text{out}} \right) + \mathbf{K}_c^d \left(\mathbf{R}^d(\theta_a)\mathbf{C}^{\text{out}} + \bar{\mathbf{R}}^d(\theta_a) + \tilde{\mathbf{R}}(\theta_a, \mathbf{C}^{\text{out}})\mathbf{C}^{\text{out}} \right) \quad (22a)$$

$$\frac{d\theta_a}{dt} = \mathbf{K}_\theta^d \left(\mathbf{R}^d(\theta_a)\mathbf{C}^{\text{out}} + \bar{\mathbf{R}}^d(\theta_a) + \tilde{\mathbf{R}}(\theta_a, \mathbf{C}^{\text{out}})\mathbf{C}^{\text{out}} \right) \quad (22b)$$

with ε representing the perturbation scalar parameter, and where :

$$\mathbf{C}^{\text{inter,d}} = \begin{pmatrix} 1 & 0 & 0 & 0 & 0 \\ 0 & 1 & 0 & 0 & 0 \\ 0 & 0 & 0 & 0 & 1 \end{pmatrix} \mathbf{C}^{\text{inter,u}} = \begin{pmatrix} C_{no}^{\text{inter}} \\ C_{no2}^{\text{inter}} \\ C_a^{\text{inter}} \end{pmatrix}, \quad \mathbf{C}^{\text{out}} = \begin{pmatrix} C_{no}^{\text{out}} \\ C_{no2}^{\text{out}} \\ C_a^{\text{out}} \end{pmatrix}, \quad (22c)$$

$$\mathbf{K}_c^d = \begin{pmatrix} 0 & 0 & 0 & -1 & 0 & -\frac{1}{2} & 0 \\ 0 & 0 & 0 & 0 & -1 & 0 & -\frac{1}{2} \\ -1 & 1 & 0 & 0 & 0 & 0 & 0 \end{pmatrix}, \quad (23)$$

$$\mathbf{K}_\theta^d = \begin{pmatrix} \frac{1}{\rho_a} & -\frac{1}{\rho_a} & -\frac{1}{\rho_a} & -\frac{1}{\rho_a} & -\frac{4}{3\rho_a} & -\frac{1}{2\rho_a} & -\frac{1}{2\rho_a} \end{pmatrix}, \quad (24)$$

$$\mathbf{R}^d(\theta_a) = \begin{pmatrix} 0 & 0 & k_{aa}(\rho_a(1-\theta_a))^{\beta_{aa}} \\ 0 & 0 & 0 \\ 0 & 0 & 0 \\ k_{sno}(\rho_a\theta_a)^{\beta_{sno}} & 0 & 0 \\ 0 & k_{sno_2}(\rho_a\theta_a)^{\beta_{sno_2}} & 0 \\ 0 & 0 & 0 \\ 0 & 0 & 0 \end{pmatrix}, \quad (25)$$

$$\tilde{\mathbf{R}}^d(\theta_a) = \begin{pmatrix} 0 \\ k_{da}(\rho_a\theta_a)^{\beta_{da}} \\ k_{oa}(\rho_a\theta_a)^{\beta_{oa}} \\ 0 \\ 0 \\ 0 \\ 0 \end{pmatrix}. \quad (26)$$

$$\tilde{\mathbf{R}}(\theta_a, \mathbf{C}^{\text{out}}) = \begin{pmatrix} 0 & 0 & 0 \\ 0 & 0 & 0 \\ 0 & 0 & 0 \\ 0 & 0 & 0 \\ 0 & 0 & 0 \\ k_{fa}(\rho_a\theta_a)^{\beta_{fa}} C_{no_2}^{\text{out}} & 0 & 0 \\ 0 & k_{fa}(\rho_a\theta_a)^{\beta_{fa}} C_{no}^{\text{out}} & 0 \end{pmatrix}, \quad (27)$$

6 Properties of the reduced models

Under adequate assumptions stated below we first solve the algebraic part of (17) and (22) exhibited previously in Section 6.2. The simplified global LNT+SCR model is exposed in section 6.3. We then show in Section 6.4 that the variables considered as coverage fractions in our model indeed do have the expected boundedness property. Finally we consider in Section 6.5 the relation of the present model with the model published in [5] which treats NO and NO₂ in an undifferentiated way.

6.1 Assumption

- According to the related litterature [12], [6], it is imposed that :

$$\beta_{ao} = \beta_{rao} = 1 \quad (28)$$

6.2 Resolution of the algebraic equations and stability issues

6.2.1 LNT reduced order model

The system is studied for the slow-time scale ($\varepsilon = 0$). (17) results in the following set of differential-algebraic equations :

$$0_5 = \frac{v_{ech}^n}{\mathcal{L}_{pn}} \left(\mathbf{C}^{\text{in}} - \mathbf{C}^{\text{inter,u}} \right) + \mathbf{K}_c^u \left(\mathbf{R}^u(\Theta) \mathbf{C}^{\text{inter,u}} + \bar{\mathbf{R}}^u(\Theta) \right) \quad (29a)$$

$$\begin{pmatrix} 1 & 0 \\ 0 & 0 \end{pmatrix} \frac{d\Theta}{dt} = \mathbf{K}_\theta^u \left(\mathbf{R}^u(\Theta) \mathbf{C}^{\text{inter,u}} + \bar{\mathbf{R}}^u(\Theta) \right) \quad (29b)$$

We set apart and solve the algebraic part of (29),

$$0_5 = \frac{v_{ech}^n}{\mathcal{L}_{pn}} \left(\mathbf{C}^{\text{in}} - \mathbf{C}^{\text{inter,u}} \right) + \mathbf{K}_c^u \left(\mathbf{R}^u(\Theta) \mathbf{C}^{\text{inter,u}} + \bar{\mathbf{R}}^u(\Theta) \right) \quad (30a)$$

$$0 = (0 \ 1) \mathbf{K}_\theta^u \left(\mathbf{R}^u(\Theta) \mathbf{C}^{\text{inter,u}} + \bar{\mathbf{R}}^u(\Theta) \right) \quad (30b)$$

recalling that $\Theta = \begin{pmatrix} \theta_n \\ \theta_o \end{pmatrix}$.

According to Tikhonov theory [21, 22], one must verify that the fast variables remain bounded even when ε tends to zero (leading to (30)), i.e that a strong stability property holds for the fast subsystem. The discussion on existence, uniqueness and stability of an equilibrium value of the fast variables, for any fixed value of the slow variables, is done in Theorems 1 and 2 below.

Theorem 1. *Assume that v_{ech}^n and C_i^{in} take on bounded and strictly positive values and that the constant parameters ρ_o , k_i^0 , \mathcal{L}_{pn} , β_i are strictly positive. Then for each value of $\theta_n \in [0, 1]$, there exists a unique solution $(\mathbf{C}^{\text{inter,u}}, \theta_o^+)$ of (30) in $\mathbb{R}_+^5 \times (0, 1)$.*

Proof. • Developing (30a), one obtains

$$\left(\frac{v_{ech}^n}{\mathcal{L}_{pn}} I - \mathbf{K}_c^u \mathbf{R}^u(\Theta) \right) \mathbf{C}^{\text{inter,u}} = \frac{v_{ech}^n}{\mathcal{L}_{pn}} \mathbf{C}^{\text{in}} + \mathbf{K}_c^u \bar{\mathbf{R}}^u(\Theta). \quad (31)$$

The matrix $\frac{v_{ech}^n}{\mathcal{L}_{pn}} I - \mathbf{K}_c^u \mathbf{R}^u(\Theta)$ is defined as the following block diagonal matrix :

$$\frac{v_{ech}^n}{\mathcal{L}_{pn}} I - \mathbf{K}_c^u \mathbf{R}^u(\Theta) = \begin{pmatrix} r_{k11} & r_{k12} & 0 & 0 & 0 \\ r_{k21} & r_{k22} & 0 & 0 & 0 \\ 0 & 0 & r_{k33} & 0 & 0 \\ 0 & 0 & 0 & r_{k44} & 0 \\ 0 & 0 & 0 & r_{k54} & r_{k55} \end{pmatrix}$$

with :

$$r_{k11} = \frac{v_{ech}^n}{\mathcal{L}_{pn}} + k_{oxno} + k_{ano}(\rho_n(1 - \theta_n))^{\beta_{ano}} \quad (32a)$$

$$r_{k12} = -k_{rno2} \quad (32b)$$

$$r_{k21} = -k_{oxno} \quad (32c)$$

$$r_{k22} = \frac{v_{ech}^n}{\mathcal{L}_{pn}} + k_{rno2} + \frac{k_{ano2}(\rho_n(1 - \theta_n))^{\beta_{ano2}}}{1 + k_{inhibno2}\theta_n} \quad (32d)$$

$$r_{k33} = \frac{v_{ech}^n}{\mathcal{L}_{pn}} + k_{ao}(\rho_o(1 - \theta_o))^{\beta_{ao}} \quad (32e)$$

$$r_{k44} = \frac{v_{ech}^n}{\mathcal{L}_{pn}} + k_{rn}(\rho_n\theta_n)^{\beta_{rn}} + k_{ra}(\rho_n\theta_n)^{\beta_{ra}} + k_{rao}(\rho_o\theta_o)^{\beta_{rao}} \quad (32f)$$

$$r_{k54} = -s_{ra}k_{ra}(\rho_n\theta_n)^{\beta_{ra}} \quad (32g)$$

$$r_{k55} = \frac{v_{ech}^n}{\mathcal{L}_{pn}} + \frac{k_{rna}}{3}(\rho_n\theta_n)^{\beta_{rna}} \quad (32h)$$

As a block diagonal matrix its determinant is such that :

$$\det \left(\frac{v_{ech}^n}{\mathcal{L}_{pn}} I - \mathbf{K}_c^u \mathbf{R}^u(\Theta) \right) = (r_{k11}r_{k22} - r_{k12}r_{k21})r_{k33}r_{k44}r_{k55} \quad (33)$$

One may notice that under the assumptions of the statement the quantity $r_{k33}r_{k44}r_{k55}$ is strictly positive. Therefore, the positiveness of (33) expression depends on the positiveness of the quantity $r_{k11}r_{k22} - r_{k12}r_{k21}$.

By a short calculation and with the help of (32a)-(32d) one observes that :

$$\begin{aligned} r_{k11}r_{k22} - r_{k12}r_{k21} &= \left(\frac{v_{ech}^n}{\mathcal{L}_{pn}} + k_{ano}(\rho_n(1 - \theta_n))^{\beta_{ano}} \right) \left(\frac{v_{ech}^n}{\mathcal{L}_{pn}} + k_{rno2} + \frac{k_{ano2}(\rho_n(1 - \theta_n))^{\beta_{ano2}}}{1 + k_{inhibno2}\theta_n} \right) \\ &+ k_{oxno} \left(\frac{v_{ech}^n}{\mathcal{L}_{pn}} + \frac{k_{ano2}(\rho_n(1 - \theta_n))^{\beta_{ano2}}}{1 + k_{inhibno2}\theta_n} \right) \end{aligned}$$

and under the assumptions of the statement $\det \left(\frac{v_{ech}^n}{\mathcal{L}_{pn}} I - \mathbf{K}_c^u \mathbf{R}^u(\Theta) \right)$ is strictly positive. As a consequence, the matrix $\frac{v_{ech}^n}{\mathcal{L}_{pn}} I - \mathbf{K}_c^u \mathbf{R}^u(\Theta)$ is invertible and from (30a) we can write $\mathbf{C}^{\text{inter},u}$ in function of θ :

$$\mathbf{C}^{\text{inter},u} = \left(\frac{v_{ech}^n}{\mathcal{L}_{pn}} I - \mathbf{K}_c^u \mathbf{R}^u(\Theta) \right)^{-1} \left(\mathbf{K}_c^u \bar{\mathbf{R}}^u(\Theta) + \frac{v_{ech}^n}{\mathcal{L}_{pn}} \mathbf{C}^{\text{in}} \right) \quad (34)$$

• We now show that θ_o can be expressed from (30b) as a function of θ_n and the input variables \mathbf{C}^{in} . For simplicity we write here :

$$\mathcal{X}(\theta_n) = k_{rn}(\rho_n\theta_n)^{\beta_{rn}} + k_{ra}(\rho_n\theta_n)^{\beta_{ra}}. \quad (35)$$

And from the assumptions in section 6.1, one obtains :

$$\frac{k_{ao}((1 - \theta_o)C_o^{\text{in}})}{v_{ech}^n + k_{ao}\mathcal{L}_{pn}(\rho_o(1 - \theta_o))^{\beta_{ao}}} - \frac{k_{rao}v_{ech}^n C_{red}^{\text{in}}\theta_o}{v_{ech}^n + \mathcal{X}(\theta_n) + k_{rao}\mathcal{L}_{pn}\rho_o\theta_o} = 0 \quad (36)$$

thus,

$$\frac{k_{ao}((1-\theta_o)C_o^{in})}{v_{ech}^n + k_{ao}\mathcal{L}_{pn}(\rho_o(1-\theta_o))^{\beta_{ao}}} = \frac{k_{rao}v_{ech}^n C_{red}^{in}\theta_o}{v_{ech}^n + \mathcal{X}(\theta_n) + k_{rao}\mathcal{L}_{pn}\rho_o\theta_o} \quad (37)$$

Let $f : (0, 1) \rightarrow \mathbb{R}$ and $g : (0, 1) \rightarrow \mathbb{R}$ be the two continuous functions

$$f(\theta_o) = \frac{k_{ao}((1-\theta_o)C_o^{in})}{v_{ech}^n + k_{ao}\mathcal{L}_{pn}(\rho_o(1-\theta_o))^{\beta_{ao}}}, \quad g(\theta_o) = \frac{k_{rao}v_{ech}^n C_{red}^{in}\theta_o}{v_{ech}^n + \mathcal{X}(\theta_n) + k_{rao}\mathcal{L}_{pn}\rho_o\theta_o}$$

Solving (37) is equivalent to the equation :

$$f(\theta_o) = g(\theta_o)$$

One verifies immediately that, when the assumptions of the statement are verified, $f(0) > 0$, $f(1) = 0$ and $g(1) > 0$, $g(0) = 0$. On the other hand, f and g are respectively decreasing and increasing functions in θ_o . Thus, there exists a unique $\theta_o = \theta_o^+(C_o^{in}, C_{red}^{in}, \theta_n)$ in $(0, 1)$ solution of (30b). Moreover, $\theta_o^+(C_o^{in}, C_{red}^{in}, \theta_n)$ is the unique positive solution of the quadratic equation deduced from (36), which permits to obtain its explicit value.

$$\theta_o^+(C_o^{in}, C_{red}^{in}, \theta_n) = \frac{v_{ech}^n(k_{rao}(v_{ech}^n + k_{ao}\mathcal{L}_{pn}\rho_o)C_{red}^{in} + k_{ao}(v_{ech}^n + \mathcal{X}(\theta_n) - \mathcal{L}_{pn}k_{rao}\rho_o)C_o^{in}) - \sqrt{\Delta}}{2k_{ao}k_{rao}\rho_o\mathcal{L}_{pn}v_{ech}^n(C_{red}^{in} - C_o^{in})} \quad (38a)$$

$$\begin{aligned} \text{with } \Delta = & (v_{ech}^n)^2(k_{rao}(v_{ech}^n + k_{ao}\mathcal{L}_{pn}\rho_o)C_{red}^{in} + k_{ao}(v_{ech}^n + \mathcal{X}(\theta_n) - \mathcal{L}_{pn}k_{rao}\rho_o)C_o^{in})^2 \\ & - 4(k_{ao}k_{rao}\rho_o\mathcal{L}_{pn}v_{ech}^n(C_{red}^{in} - C_o^{in}))(k_{ao}v_{ech}^n C_o^{in}(v_{ech}^n + \mathcal{X}(\theta_n))) \end{aligned} \quad (38b)$$

This achieves the proof of Theorem 1. \square

Stability issues are considered in the following result.

Theorem 2. *Assume that v_{ech}^n , C_i^{in} and C_i^{inter} take on bounded and strictly positive values and that the constant parameters ρ_o , k_i^0 , \mathcal{L}_{pn} , β_i are strictly positive. Then for any value of $\theta_n \in (0, 1)$, the equilibrium point exhibited in Theorem 1 is asymptotically stable.*

Proof. Let \mathcal{J} be the Jacobian matrix of the fast subsystem evaluated at the equilibrium point $(\mathbf{C}^{inter, \mathbf{u}}, \theta_o^+)$ and defined from (30) as :

$$\mathcal{J} = \begin{pmatrix} -\frac{v_{ech}^n}{\mathcal{L}_{pn}}I_5 + \mathbf{K}_c^{\mathbf{u}}\mathbf{R}^{\mathbf{u}}(\Theta) & \mathbf{K}_c^{\mathbf{u}}(\nabla_{\theta_o}\mathbf{R}^{\mathbf{u}}(\Theta)\mathbf{C}^{inter, \mathbf{u}} + \nabla_{\theta_o}\bar{\mathbf{R}}^{\mathbf{u}}(\Theta)) \\ (0 \ 1)\mathbf{K}_\theta^{\mathbf{u}}\mathbf{R}^{\mathbf{u}}(\Theta) & (0 \ 1)\mathbf{K}_\theta^{\mathbf{u}}(\nabla_{\theta_o}\mathbf{R}^{\mathbf{u}}(\Theta)\mathbf{C}^{inter, \mathbf{u}} + \nabla_{\theta_o}\bar{\mathbf{R}}^{\mathbf{u}}(\Theta)) \end{pmatrix} \quad (39)$$

where ∇_{θ_o} denotes the differential operator at θ_o . One will show that the spectrum of \mathcal{J} lies in the open left half plane. From (17c) to (21) one obtains :

$$\mathcal{J} = \begin{pmatrix} J_a & 0_{2 \times 4} \\ 0_{4 \times 2} & J_b \end{pmatrix} \quad (40)$$

with,

$$J_a = \begin{pmatrix} j_{a11} & j_{a12} \\ j_{a21} & j_{a22} \end{pmatrix} \quad (41a)$$

$$J_b = \begin{pmatrix} j_{b11} & 0 & 0 & j_{b14} \\ 0 & j_{b22} & 0 & j_{b24} \\ 0 & j_{b32} & j_{b33} & 0 \\ j_{b41} & j_{b42} & 0 & j_{b44} \end{pmatrix} \quad (41b)$$

and where the j_{ai} and j_{bi} are defined hereafter:

$$j_{a11} = -\frac{v_{ech}^n}{\mathcal{L}_{pn}} - k_{oxno} - k_{ano}(\rho_n(1 - \theta_n))^{\beta_{ano}} \quad (42a)$$

$$j_{a12} = k_{rno2} \quad (42b)$$

$$j_{a21} = k_{oxno} \quad (42c)$$

$$j_{a22} = -\frac{v_{ech}^n}{\mathcal{L}_{pn}} - k_{rno2} - \frac{k_{ano2}(\rho_n(1 - \theta_n))^{\beta_{ano2}}}{1 + k_{inhibno2}\theta_n} \quad (42d)$$

$$j_{b11} = -\frac{v_{ech}^n}{\mathcal{L}_{pn}} - k_{ao}(\rho_o(1 - \theta_o))^{\beta_{ao}} \quad (42e)$$

$$j_{b14} = k_{ao}\beta_{ao}\rho_o^{\beta_{ao}}(1 - \theta_o)^{\beta_{ao}-1}C_o^{inter} \quad (42f)$$

$$j_{b22} = -\frac{v_{ech}^n}{\mathcal{L}_{pn}} - k_{rn}(\rho_n\theta_n)^{\beta_{rn}} - k_{ra}(\rho_n\theta_n)^{\beta_{ra}} - k_{rao}(\rho_o\theta_o)^{\beta_{rao}} \quad (42g)$$

$$j_{b24} = -k_{rao}\beta_{rao}\rho_o^{\beta_{rao}}\theta_o^{\beta_{rao}-1}C_{red}^{inter} \quad (42h)$$

$$j_{b32} = s_{ra}k_{ra}(\rho_n\theta_n)^{\beta_{ra}} \quad (42i)$$

$$j_{b33} = -\frac{v_{ech}^n}{\mathcal{L}_{pn}} - \frac{k_{rna}}{3}(\rho_n\theta_n)^{\beta_{rna}} \quad (42j)$$

$$j_{b41} = \frac{k_{ao}}{\rho_o}(\rho_o(1 - \theta_o))^{\beta_{ao}} \quad (42k)$$

$$j_{b42} = -\frac{k_{rao}}{\rho_o}(\rho_o\theta_o)^{\beta_{rao}} \quad (42l)$$

$$j_{b44} = -k_{ao}\beta_{ao}(\rho_o(1 - \theta_o))^{\beta_{ao}-1}C_o^{inter} - k_{rao}\beta_{rao}(\rho_o\theta_o)^{\beta_{rao}-1}C_{red}^{inter} \quad (42m)$$

Notice that the signs of these quantities are easily deduced from the fact that all the quantities involved are positive. This property will be used afterwards.

- By a short calculation one observes that :

$$\begin{aligned} \det(J_a) &= \left(\frac{v_{ech}^n}{\mathcal{L}_{pn}} + k_{ano}(\rho_n(1 - \theta_n))^{\beta_{ano}}\right)\left(\frac{v_{ech}^n}{\mathcal{L}_{pn}} + k_{rno2} + \frac{k_{ano2}(\rho_n(1 - \theta_n))^{\beta_{ano2}}}{1 + k_{inhibno2}\theta_n}\right) \\ &\quad + k_{oxno}\left(\frac{v_{ech}^n}{\mathcal{L}_{pn}} + \frac{k_{ano2}(\rho_n(1 - \theta_n))^{\beta_{ano2}}}{1 + k_{inhibno2}\theta_n}\right) \\ \text{tr}(J_a) &= -2\frac{v_{ech}^n}{\mathcal{L}_{pn}} - k_{oxno} - k_{ano}(\rho_n(1 - \theta_n))^{\beta_{ano}} - k_{rno2} - \frac{k_{ano2}(\rho_n(1 - \theta_n))^{\beta_{ano2}}}{1 + k_{inhibno2}\theta_n} \end{aligned}$$

and under the assumptions of the statement $\det(J_a) > 0$ and $\text{tr}(J_a) < 0$. Thus, J_a is Hurwitz.

• On the other hand, we have that :

$$\begin{aligned} \det(\lambda I_4 - J_b) &= \begin{vmatrix} \lambda - j_{b11} & 0 & 0 & -j_{b14} \\ 0 & \lambda - j_{b22} & 0 & -j_{b24} \\ 0 & -j_{b32} & \lambda - j_{b33} & 0 \\ -j_{b41} & -j_{b42} & 0 & \lambda - j_{b44} \end{vmatrix} \\ &= (\lambda - j_{b33})((\lambda - j_{b11})(\lambda - j_{b22})(\lambda - j_{b44}) - (\lambda - j_{b22})j_{b14}j_{b41} - (\lambda - j_{b11})j_{b24}j_{b42}) \\ &= (\lambda - j_{b33})\mathcal{P}(\lambda) \end{aligned}$$

with

$$\mathcal{P}(\lambda) = \lambda^3 + p_1\lambda^2 + p_2\lambda + p_3$$

and where,

$$p_1 = -(j_{b11} + j_{b22} + j_{b44}) \quad (43a)$$

$$p_2 = (j_{b11}j_{b22} - j_{b14}j_{b41} - j_{b24}j_{b42} + j_{b44}(j_{b11} + j_{b22})) \quad (43b)$$

$$p_3 = -(j_{b11}j_{b22}j_{b44} + j_{b22}j_{b14}j_{b41} + j_{b11}j_{b24}j_{b42}) \quad (43c)$$

Under the assumptions of the statement, j_{b33} is strictly negative (see (42j)), thus, all one has to do is to show that \mathcal{P} has all its roots in the left half plane.

The Routh-Hurwitz criterion requires the strict positivity of p_1 , p_2 , p_3 and $(p_2p_1 - p_3)$ for the stability of \mathcal{P} . This is what we prove in the sequel. Under the assumptions of the statement and with the help of (42), one is able to say that $p_1 > 0$, p_2 and $p_3 > 0$. Then, from (43a) to (43c), one obtains :

$$\begin{aligned} p_2p_1 - p_3 &= -j_{b11}j_{b22}(j_{b11} + j_{b22}) + j_{b14}j_{b41}(j_{b11} + 2j_{b22} + j_{b44}) + j_{b24}j_{b42}(j_{b22} + 2j_{b11} + j_{b44}) \\ &\quad - (j_{b11} + j_{b22} + j_{b44})(j_{b44}(j_{b11} + j_{b22})) \end{aligned} \quad (44)$$

Observing that :

$$\begin{aligned} j_{b44} &= \frac{1}{\rho_o} (-j_{b14} + j_{b24}) \\ j_{b11} &= -\frac{v_{ech}^n}{\mathcal{L}_{pn}} - j_{b41}\rho_o \\ j_{b22} &= -\frac{v_{ech}^n}{\mathcal{L}_{pn}} - \mathcal{X}(\theta_n) + j_{b42}\rho_o, \text{ where } \mathcal{X}(\theta_n) \text{ is defined in (35)} \end{aligned}$$

we develop and simplify (44). Then, after reordering each term, this leads to :

$$\begin{aligned} p_2p_1 - p_3 &= -j_{b11}j_{b22}(j_{b11} + j_{b22}) \\ &\quad + j_{b14} \left(j_{b42} - \frac{1}{\rho_o} \left(\frac{v_{ech}^n}{\mathcal{L}_{pn}} + \mathcal{X}(\theta_n) \right) \right) \left(-2\frac{v_{ech}^n}{\mathcal{L}_{pn}} - \mathcal{X}(\theta_n) + j_{b42}\rho_o + j_{b44} \right) \\ &\quad + j_{b24} \left(j_{b41} + \frac{1}{\rho_o} \frac{v_{ech}^n}{\mathcal{L}_{pn}} \right) \left(-2\frac{v_{ech}^n}{\mathcal{L}_{pn}} - \mathcal{X}(\theta_n) - j_{b41}\rho_o + j_{b44} \right) \\ &\quad + \left(j_{b44} \frac{v_{ech}^n}{\mathcal{L}_{pn}} + j_{b24} \frac{\mathcal{X}(\theta_n)}{\rho_o} \right) (j_{b11} + j_{b22} + j_{b44}) \end{aligned} \quad (45)$$

The proof of this formula is shown in Appendix B. Under the assumptions of the statement and with the help of (42), one can verify that :

$$\begin{aligned}
 & -j_{b11}j_{b22}(j_{b11} + j_{b22}) > 0 \\
 & j_{b14} \left(j_{b42} - \frac{1}{\rho_o} \left(\frac{v_{ech}^n}{\mathcal{L}_{pn}} + \mathcal{X}(\theta_n) \right) \right) < 0 \\
 & \left(-2 \frac{v_{ech}^n}{\mathcal{L}_{pn}} - \mathcal{X}(\theta_n) + j_{b42}\rho_o + j_{b44} \right) < 0 \\
 & j_{b24} \left(j_{b41} + \frac{1}{\rho_o} \frac{v_{ech}^n}{\mathcal{L}_{pn}} \right) < 0 \\
 & \left(-2 \frac{v_{ech}^n}{\mathcal{L}_{pn}} - \mathcal{X}(\theta_n) - j_{b41}\rho_o + j_{b44} \right) < 0 \\
 & \left(j_{b44} \frac{v_{ech}^n}{\mathcal{L}_{pn}} + j_{b24} \frac{\mathcal{X}(\theta_n)}{\rho_o} \right) < 0 \\
 & (j_{b11} + j_{b22} + j_{b44}) < 0
 \end{aligned}$$

Thus, comparing the sign of each term leads to $p_2p_1 - p_3 > 0$. Then, from Routh-Hurwitz criterion, \mathcal{P} is Hurwitz and as a conclusion \mathcal{J} is asymptotically stable. This achieves the proof of Theorem 2. \square

Then, it yields the following **LNT reduced order model**

$$\rho_n \dot{\theta}_n = k_{ano2} \frac{C_{no2}^{inter} (\rho_n (1 - \theta_n))^{\beta_{ano2}}}{1 + k_{inhibno2} \theta_n} - k_{dno2} (\rho_n \theta_n)^{\beta_{dno2}} + k_{ano} (\rho_n (1 - \theta_n))^{\beta_{ano}} C_{no}^{inter} \quad (46a)$$

$$- s_{rn} k_{rn} (\rho_n \theta_n)^{\beta_{rn}} C_{red}^{inter} - s_{ra} k_{ra} (\rho_n \theta_n)^{\beta_{ra}} C_{red}^{inter} - \frac{k_{rna}}{4} (\rho_n \theta_n)^{\beta_{rna}} C_a^{inter}$$

$$\theta_o = \theta_o^+(C_o^{in}, C_{red}^{in}, \theta_n), \quad \text{see (38)} \quad (46b)$$

$$C_{no}^{inter} = \frac{v_{ech}^n C_{no}^{in} + k_{rno2} \mathcal{L}_{pn} C_{no2}^{inter}}{v_{ech}^n + k_{oxno} \mathcal{L}_{pn} + k_{ano} \mathcal{L}_{pn} (\rho_n (1 - \theta_n))^{\beta_{ano}}} \quad (46c)$$

$$C_{no2}^{inter} = \frac{(1 + k_{inhibno2} \theta_n) (v_{ech}^n C_{no2}^{in} + k_{dno2} \mathcal{L}_{pn} (\rho_n \theta_n)^{\beta_{dno2}} + k_{oxno} \mathcal{L}_{pn} C_{no}^{inter})}{(1 + k_{inhibno2} \theta_n) (v_{ech}^n + k_{rno2} \mathcal{L}_{pn}) + k_{ano2} \mathcal{L}_{pn} (\rho_n (1 - \theta_n))^{\beta_{ano2}}} \quad (46d)$$

$$C_o^{inter} = \frac{v_{ech}^n C_o^{in}}{v_{ech}^n + k_{ao} \mathcal{L}_{pn} \rho_o (1 - \theta_o)} \quad (46e)$$

$$C_{red}^{inter} = \frac{v_{ech}^n C_{red}^{in}}{v_{ech}^n + k_{rn} \mathcal{L}_{pn} (\rho_n \theta_n)^{\beta_{rn}} + k_{ra} \mathcal{L}_{pn} (\rho_n \theta_n)^{\beta_{ra}} + k_{rao} \mathcal{L}_{pn} (\rho_o \theta_o)^{\beta_{rao}}} \quad (46f)$$

$$C_a^{inter} = \frac{s_{ra} k_{ra} \mathcal{L}_{pn} C_{red}^{inter} (\rho_n \theta_n)^{\beta_{ra}}}{v_{ech}^n + k_{rna} \mathcal{L}_{pn} (\rho_n \theta_n)^{\beta_{rna}}} \quad (46g)$$

6.2.2 SCR reduced order model

Let us consider the equation set (22), with $\varepsilon = 0$ that is :

$$0_3 = \frac{v_{ech}^s}{\mathcal{L}_{scr}} \left(\mathbf{C}^{inter,d} - \mathbf{C}^{out} \right) + \mathbf{K}_c^d \left(\mathbf{R}^d(\theta_a) \mathbf{C}^{out} + \bar{\mathbf{R}}^d(\theta_a) + \tilde{\mathbf{R}}(\theta_a, \mathbf{C}^{out}) \mathbf{C}^{out} \right) \quad (47a)$$

$$\frac{d\theta_a}{dt} = \mathbf{K}_\theta^d \left(\mathbf{R}^d(\theta_a) \mathbf{C}^{out} + \bar{\mathbf{R}}^d(\theta_a) + \tilde{\mathbf{R}}(\theta_a, \mathbf{C}^{out}) \mathbf{C}^{out} \right) \quad (47b)$$

We set apart and solve the algebraic part of (47),

$$0_3 = \frac{v_{ech}^s}{\mathcal{L}_{scr}} \left(\mathbf{C}^{inter,d} - \mathbf{C}^{out} \right) + \mathbf{K}_c^d \left(\mathbf{R}^d(\theta_a) \mathbf{C}^{out} + \bar{\mathbf{R}}^d(\theta_a) + \tilde{\mathbf{R}}(\theta_a, \mathbf{C}^{out}) \mathbf{C}^{out} \right) \quad (48)$$

Contrary to the LNT, system (48) is not linear with respect to the output concentrations gathered in the vector defined previously in (22c),

$$\mathbf{C}^{out} = \begin{pmatrix} C_{no}^{out} \\ C_{no_2}^{out} \\ C_a^{out} \end{pmatrix} \quad (49)$$

However, stability property, existence and uniqueness of solutions also hold as stated now.

Theorem 3. *Assume that v_{ech}^s and C_i^{in} take on bounded and strictly positive values and that the constant parameters ρ_o , k_i^0 , \mathcal{L}_{scr} , β_i are strictly positive. Then for each value of $\theta_a \in [0, 1]$, there exists a unique solution \mathbf{C}^{out} of (48) in \mathbb{R}_+^3 .*

Proof. The fully developed form of (47) leads to the resolution of the following nonlinear equation system :

$$0 = \frac{v_{ech}^s}{\mathcal{L}_{scr}} (C_{no}^{inter} - C_{no}^{out}) - k_{sno}(\rho_a \theta_a)^{\beta_{sno}} C_{no}^{out} - \frac{k_{fa}}{2} C_{no}^{out} C_{no_2}^{out} (\rho_a \theta_a)^{\beta_{fa}} \quad (50a)$$

$$0 = \frac{v_{ech}^s}{\mathcal{L}_{scr}} (C_{no_2}^{inter} - C_{no_2}^{out}) - k_{sno_2}(\rho_a \theta_a)^{\beta_{sno_2}} C_{no_2}^{out} - \frac{k_{fa}}{2} C_{no}^{out} C_{no_2}^{out} (\rho_a \theta_a)^{\beta_{fa}} \quad (50b)$$

$$0 = \frac{v_{ech}^s}{\mathcal{L}_{scr}} (C_a^{in} - C_a^{out}) - k_{aa}(\rho_a(1 - \theta_a))^{\beta_{aa}} C_a^{out} + k_{da}(\rho_a \theta_a)^{\beta_{da}} \quad (50c)$$

Developing (50b) with the help of (50a) yields:

$$a(C_{no_2}^{out})^2 + bC_{no_2}^{out} + c = 0 \quad (51)$$

where

$$a = -\frac{k_{fa}}{2} \mathcal{L}_{scr} (\rho_a \theta_a)^{\beta_{fa}} (v_{ech}^s + k_{sno_2} \mathcal{L}_{scr} (\rho_a \theta_a)^{\beta_{sno_2}}) \quad (52a)$$

$$b = -(v_{ech}^s + k_{sno_2} \mathcal{L}_{scr} (\rho_a \theta_a)^{\beta_{sno_2}}) (v_{ech}^s + k_{sno} \mathcal{L}_{scr} (\rho_a \theta_a)^{\beta_{sno}}) + v_{ech}^s \frac{k_{fa}}{2} \mathcal{L}_{scr} (\rho_a \theta_a)^{\beta_{fa}} (C_{no_2}^{inter} - C_{no}^{inter}) \quad (52b)$$

$$c = v_{ech}^s C_{no_2}^{inter} (v_{ech}^s + k_{sno} \mathcal{L}_{scr} (\rho_a \theta_a)^{\beta_{sno}}) \quad (52c)$$

From the assumptions one obtains that $a < 0$ and $c > 0$. As a consequence, (51) admits two solutions of different signs. Thus there exists a unique solution $C_{no_2}^{out,+}(C_{no}^{inter}, C_{no_2}^{inter}, \theta_a)$ of (51) in \mathbb{R}^+ whose expression is given by,

$$C_{no_2}^{out,+} = \frac{-b - \sqrt{\Delta}}{2a}, \quad \Delta = b^2 - 4ac \quad (52d)$$

(50b) and (50c) provide directly the values of C_{no}^{out} and C_a^{out} . This achieves the proof of Theorem 3. \square

Stability issue is considered in the following result.

Theorem 4. *Assume that v_{ech}^s , C_i^{in} and C_i^{out} take on bounded and strictly positive values and that the constant parameters ρ_a , k_i^0 , \mathcal{L}_{scr} , β_i are strictly positive. Then for any value of $\theta_a \in (0, 1)$, the equilibrium point exhibited in Theorem 3 is asymptotically stable.*

Proof. Let \mathcal{J} be the Jacobian matrix of the fast subsystem evaluated at the equilibrium point \mathbf{C}^{out} and defined from (48) as :

$$\mathcal{J} = -\frac{v_{ech}^s}{\mathcal{L}_{scr}} I_3 + \mathbf{K}_c^d(\mathbf{R}^d(\theta_a)) + \nabla_{C^{out}} \tilde{\mathbf{R}}(\theta_a, \mathbf{C}^{out}) \mathbf{C}^{out} \quad (53)$$

where $\nabla_{C^{out}}$ denotes the differential operator at C^{out} . One will show that the spectrum of \mathcal{J} lies in the open left half plane. From (22c) to (27) one obtains :

$$\mathcal{J} = \begin{pmatrix} J & 0_{2 \times 1} \\ 0_{1 \times 2} & j_{33} \end{pmatrix} \quad (54)$$

with

$$J = \begin{pmatrix} j_{11} & j_{12} \\ j_{21} & j_{22} \end{pmatrix} \quad (55)$$

and where the j_i are defined hereafter:

$$j_{11} = -\frac{v_{ech}^s}{\mathcal{L}_{scr}} - k_{sno}(\rho_a \theta_a)^{\beta_{sno}} - \frac{k_{fa}}{2}(\rho_a \theta_a)^{\beta_{fa}} C_{no_2}^{out} \quad (56a)$$

$$j_{12} = -\frac{k_{fa}}{2}(\rho_a \theta_a)^{\beta_{fa}} C_{no}^{out} \quad (56b)$$

$$j_{21} = -\frac{k_{fa}}{2}(\rho_a \theta_a)^{\beta_{fa}} C_{no_2}^{out} \quad (56c)$$

$$j_{22} = -\frac{v_{ech}^s}{\mathcal{L}_{scr}} - k_{sno_2}(\rho_a \theta_a)^{\beta_{sno_2}} - \frac{k_{fa}}{2}(\rho_a \theta_a)^{\beta_{fa}} C_{no}^{out} \quad (56d)$$

$$j_{33} = -\frac{v_{ech}^s}{\mathcal{L}_{scr}} - k_{aa}(\rho_a(1 - \theta_a))^{\beta_{aa}} \quad (56e)$$

As a block diagonal matrix $\text{spec}(\mathcal{J}) = \text{spec}(J) \cup \{j_{33}\}$. The quantity j_{33} is negative, thus, it remains to show that $\text{spec}(J) \in \{z \in \mathbb{C}/\text{Re}(z) < 0\}$. By a short calculation one observes that :

$$\begin{aligned} \det(J) &= j_{11}j_{22} - j_{21}j_{12} \\ &= \left(\frac{v_{ech}^s}{\mathcal{L}_{scr}} + k_{sno}(\rho_a \theta_a)^{\beta_{sno}}\right) \left(\frac{v_{ech}^s}{\mathcal{L}_{scr}} + k_{sno_2}(\rho_a \theta_a)^{\beta_{sno_2}} + \frac{k_{fa}}{2}(\rho_a \theta_a)^{\beta_{fa}} C_{no}^{out}\right) \\ &\quad + \frac{k_{fa}}{2}(\rho_a \theta_a)^{\beta_{fa}} \left(\frac{v_{ech}^s}{\mathcal{L}_{scr}} + k_{sno_2}(\rho_a \theta_a)^{\beta_{sno_2}}\right) C_{no_2}^{out} \end{aligned} \quad (57)$$

Thus, under the assumptions of the statement one is able to say that $\det(J) > 0$, $\text{tr}(J) < 0$ and as a conclusion, \mathcal{J} is Hurwitz. This achieves the proof of Theorem 4 \square

We finally ended up with the following **SCR reduced order model** :

$$\rho_a \dot{\theta}_a = k_{aa}(\rho_a(1 - \theta_a))^{\beta_{aa}} C_a^{\text{out}} - k_{da}(\rho_a \theta_a)^{\beta_{da}} - k_{oa}(\rho_a \theta_a)^{\beta_{oa}} - \frac{4}{3} k_{sno_2}(\rho_a \theta_a)^{\beta_{sno_2}} C_{no_2}^{\text{out}} \quad (58a)$$

$$- k_{sno}(\rho_a \theta_a)^{\beta_{sno}} C_{no}^{\text{out}} - k_{fa}(\rho_a \theta_a)^{\beta_{fa}} C_{no}^{\text{out}} C_{no_2}^{\text{out}}$$

$$C_{no_2}^{\text{out}} = C_{no_2}^{\text{out},+}(C_{no}^{\text{inter}}, C_{no_2}^{\text{inter}}, \theta_a), \text{ see (52)} \quad (58b)$$

$$C_{no}^{\text{out}} = \frac{v_{ech}^s C_{no}^{\text{inter}}}{v_{ech}^s + k_{sno} \mathcal{L}_{scr}(\rho_a \theta_a)^{\beta_{sno}} + \frac{k_{fa}}{2} \mathcal{L}_{scr}(\rho_a \theta_a)^{\beta_{fa}} C_{no_2}^{\text{out}}} \quad (58c)$$

$$C_a^{\text{out}} = \frac{v_{ech}^s C_a^{\text{inter}} + k_{da} \mathcal{L}_{scr}(\rho_a \theta_a)^{\beta_{da}}}{v_{ech} + k_{aa} \mathcal{L}_{scr}(\rho_a(1 - \theta_a))^{\beta_{aa}}} \quad (58d)$$

6.3 Global reduced system

Due to the explicit resolution of the algebraic part of both subsystems, the reduced system turns out to be composed of a two-dimensional ode, namely,

$$\rho_n \dot{\theta}_n = k_{ano_2} \frac{C_{no_2}^{\text{inter}}(\rho_n(1 - \theta_n))^{\beta_{ano_2}}}{1 + k_{inhibno_2} \theta_n} - k_{dno_2}(\rho_n \theta_n)^{\beta_{dno_2}} + k_{ano}(\rho_n(1 - \theta_n))^{\beta_{ano}} C_{no}^{\text{inter}} \quad (59a)$$

$$- s_{rn} k_{rn}(\rho_n \theta_n)^{\beta_{rn}} C_{red}^{\text{inter}} - s_{ra} k_{ra}(\rho_n \theta_n)^{\beta_{ra}} C_{red}^{\text{inter}} - \frac{k_{rna}}{4}(\rho_n \theta_n)^{\beta_{rna}} C_a^{\text{inter}}$$

$$\rho_a \dot{\theta}_a = k_{aa}(\rho_a(1 - \theta_a))^{\beta_{aa}} C_a^{\text{out}} - k_{da}(\rho_a \theta_a)^{\beta_{da}} - k_{oa}(\rho_a \theta_a)^{\beta_{oa}} - \frac{4}{3} k_{sno_2}(\rho_a \theta_a)^{\beta_{sno_2}} C_{no_2}^{\text{out}} \quad (59b)$$

$$- k_{sno}(\rho_a \theta_a)^{\beta_{sno}} C_{no}^{\text{out}} - k_{fa}(\rho_a \theta_a)^{\beta_{fa}} C_{no}^{\text{out}} C_{no_2}^{\text{out}}$$

where

$$\theta_o = \theta_o^+(C_o^{in}, C_{red}^{in}, \theta_n), \quad \text{see (38)} \quad (59c)$$

$$C_{no}^{inter} = \frac{v_{ech}^n C_{no}^{in} + k_{rno_2} \mathcal{L}_{pn} C_{no_2}^{inter}}{v_{ech}^n + k_{oxno} \mathcal{L}_{pn} + k_{ano} \mathcal{L}_{pn} (\rho_n (1 - \theta_n))^{\beta_{ano}}} \quad (59d)$$

$$C_{no_2}^{inter} = \frac{(1 + k_{inhibno_2} \theta_n)(v_{ech}^n C_{no_2}^{in} + k_{dno_2} \mathcal{L}_{pn} (\rho_n \theta_n)^{\beta_{dno_2}} + k_{oxno} \mathcal{L}_{pn} C_{no}^{inter})}{(1 + k_{inhibno_2} \theta_n)(v_{ech}^n + k_{rno_2} \mathcal{L}_{pn}) + k_{ano_2} \mathcal{L}_{pn} (\rho_n (1 - \theta_n))^{\beta_{ano_2}}} \quad (59e)$$

$$C_o^{inter} = \frac{v_{ech}^n C_o^{in}}{v_{ech}^n + k_{ao} \mathcal{L}_{pn} \rho_o (1 - \theta_o)} \quad (59f)$$

$$C_{red}^{inter} = \frac{v_{ech}^n C_{red}^{in}}{v_{ech}^n + k_{rn} \mathcal{L}_{pn} (\rho_n \theta_n)^{\beta_{rn}} + k_{ra} \mathcal{L}_{pn} (\rho_n \theta_n)^{\beta_{ra}} + k_{rao} \mathcal{L}_{pn} (\rho_o \theta_o)^{\beta_{rao}}} \quad (59g)$$

$$C_a^{inter} = \frac{s_{ra} k_{ra} \mathcal{L}_{pn} C_{red}^{inter} (\rho_n \theta_n)^{\beta_{ra}}}{v_{ech}^n + k_{rna} \mathcal{L}_{pn} (\rho_n \theta_n)^{\beta_{rna}}} \quad (59h)$$

$$C_{no_2}^{out} = C_{no_2}^{out,+}(C_{no}^{inter}, C_{no_2}^{inter}, \theta_a), \quad \text{see (52)} \quad (59i)$$

$$C_{no}^{out} = \frac{v_{ech}^s C_{no}^{inter}}{v_{ech}^s + k_{sno} \mathcal{L}_{scr} (\rho_a \theta_a)^{\beta_{sno}} + \frac{k_{fa}}{2} \mathcal{L}_{scr} (\rho_a \theta_a)^{\beta_{fa}} C_{no_2}^{out}} \quad (59j)$$

$$C_a^{out} = \frac{v_{ech}^s C_a^{inter} + k_{da} \mathcal{L}_{scr} (\rho_a \theta_a)^{\beta_{da}}}{v_{ech}^s + k_{aa} \mathcal{L}_{scr} (\rho_a (1 - \theta_a))^{\beta_{aa}}} \quad (59k)$$

Its state variable is (θ_n, θ_a) , composed thus of the coverage fractions of NO_x in the LNT and ammonia in the SCR. Notice the triangular structure in (59), reminiscent of the upstream-downstream structure of the device : θ_n evolves independently of θ_a .

6.4 Boundedness of the coverage fractions

Being supposed to represent coverage fractions, the variables θ_n and θ_a should take on values belonging to the interval $[0, 1]$ at any time. Thus it is important to verify that the reduced model exhibits such a property. This is what we do now.

Theorem 5. *Consider equation (59). Assume that the variables $v_{ech}^n, v_{ech}^s, C_i^{in}$ are bounded and take on strictly positive values, and that the kinetic constants $\rho, k_i^0, \mathcal{L}_{pn}, \mathcal{L}_{scr}, \beta_i$ are strictly positive. If at the initial time $t = 0$,*

$$0 \leq \theta_n(0) \leq 1, \quad 0 \leq \theta_a(0) \leq 1$$

then the same inequalities are fulfilled for any t . Moreover, the same property is valid with strict inequalities.

Proof. The assumptions yield directly,

$$\begin{cases} \dot{\theta}_i > 0, & \text{if } \theta_i = 0 \\ \dot{\theta}_i < 0, & \text{if } \theta_i = 1, \text{ for } i = a, n \end{cases}$$

The proof of Theorem 5 then comes from direct application of the following Lemma.

Lemma 1. *Let $f : \mathbb{R}^+ \times \mathbb{R}^n \rightarrow \mathbb{R}^n$ be a continuous function and $\Omega = [0, 1]^n$. Assume that there exists $c > 0$ such that for any $t \in \mathbb{R}^+$, for any $x \in \Omega$, for any $i \in \{1, \dots, n\}$,*

$$\begin{cases} x_i = 0, & \text{if } f_i(t, x) > c, \\ x_i = 1, & \text{if } f_i(t, x) < -c. \end{cases}$$

Then, denoting $\bar{\Omega}$ the closure of Ω , if there exists t_0 such that $x(t_0) \in \Omega$ (resp. $\bar{\Omega}$), then $x(t) \in \Omega$ (resp. $\bar{\Omega}$) for any $t > t_0$, where $x(t)$ is a solution of the ode $\dot{x}(t) = f(t, x)$, $x(t_0) = x_0$

This achieves the proof of Theorem 5. □

The algebro-differential structure of system (59) permits to deduce from Theorem 5 a result of positivity of the concentrations.

Corollary 1. *Under the hypotheses of Theorem 5, for any $t > 0$ the components of the concentration vectors $\mathbf{C}^{\text{inter}, \mathbf{u}}$ defined in (17c) and \mathbf{C}^{out} defined in (22c) are strictly positive. The value of θ_o lies in $(0, 1)$.*

Proof. The proof of Corollary 1 is evident from Theorem 1 and Theorem 3. □

6.5 Further reduction of the models

The aim of this part is to show that under adequate assumptions, the models with NO/NO₂ differentiation developed here can be further reduced, leading to a model similar to the one presented in [5]. Euro 6 standards only lay down restrictions on global NO_x emissions. Currently the sensors available on the vehicles are NO_x sensors, providing global information on the concentration of NO+NO₂. Even for calibrations, NO and NO₂ measurements are not always at disposal, it is thus meaningful to develop a model with an aggregated NO_x species.

6.5.1 Assumptions

Let us define the aggregated NO_x species as :

$$C_{nox} = C_{no} + C_{no_2} \quad (60)$$

The following assumptions are considered :

- It is assumed that the exhaust gas NO_x only corresponds to NO species, i.e :

$$C_{no}^{\text{in}} = C_{nox}^{\text{in}}, \quad C_{no_2}^{\text{in}} = 0. \quad (61)$$

Indeed, NO_x in the exhaust gas exits the engine in majority under the form of NO, the NO₂ essentially originating from the oxidation reaction taking place at the beginning of the storage process in the NO_x trap.

- We assume that the oxidation mechanism of NO species is dominant (see (9a)) and that no NO species is created from the existing reactions, i.e :

$$k_{oxno} \gg \frac{v_{ech}^n}{\mathcal{L}_{pm}}, \quad k_{ano} \quad k_{rno_2} = 0. \quad (62)$$

6.5.2 Resulting model

The result of the reduction process is given by the following Theorem :

Theorem 6. Assume (61) and (62). Then, considering C_{nox} as defined in (60), the solutions of system (59) verify :

$$\begin{aligned} \rho_n \dot{\theta}_n &= k_{anox} \frac{C_{nox}^{inter} (\rho_n (1 - \theta_n))^{\beta_{anox}}}{1 + k_{inhibnox} \theta_n} - k_{dnox} (\rho_n \theta_n)^{\beta_{dnox}} - s_{rnox} k_{rnox} (\rho_n \theta_n)^{\beta_{rnox}} C_{red}^{inter} \\ &\quad - s_{ra} k_{raox} (\rho_n \theta_n)^{\beta_{raox}} C_{red}^{inter} - \frac{k_{rnaox}}{4} (\rho_n \theta_n)^{\beta_{rnaox}} C_a^{inter} \end{aligned} \quad (63a)$$

$$\rho_a \dot{\theta}_a = k_{aaox} (\rho_a (1 - \theta_a))^{\beta_{aaox}} C_a^{out} - k_{daox} (\rho_a \theta_a)^{\beta_{daox}} - k_{snox} (\rho_a \theta_a)^{\beta_{snox}} C_{nox}^{out} - k_{oaox} (\rho_a \theta_a)^{\beta_{oaox}} \quad (63b)$$

where

$$C_{nox}^{inter} = \frac{(1 + k_{inhibnox} \theta_n) (v_{ech}^n C_{nox}^{in} + k_{dnox} \mathcal{L}_{pn} (\rho_n \theta_n)^{\beta_{dnox}})}{v_{ech}^n (1 + k_{inhibnox} \theta_n) + k_{anox} \mathcal{L}_{pn} (\rho_n (1 - \theta_n))^{\beta_{anox}}} \quad (63c)$$

$$C_{red}^{inter} = \frac{v_{ech}^n C_{red}^{in}}{v_{ech}^n + k_{rnox} \mathcal{L}_{pn} (\rho_n \theta_n)^{\beta_{rnox}} + k_{raox} \mathcal{L}_{pn} (\rho_n \theta_n)^{\beta_{raox}} + k_{raox} \mathcal{L}_{pn} (\rho_o \theta_o)^{\beta_{raox}}} \quad (63d)$$

$$C_a^{inter} = \frac{s_{ra} k_{raox} \mathcal{L}_{pn} C_{red}^{inter} (\rho_n \theta_n)^{\beta_{raox}}}{v_{ech}^n + k_{rnaox} \mathcal{L}_{pn} (\rho_n \theta_n)^{\beta_{rnaox}}} \quad (63e)$$

$$\theta_o = \theta_o^+ (C_o^{in}, C_{red}^{in}, \theta_n), \quad \text{see (38)} \quad (63f)$$

$$C_{nox}^{out} = \frac{v_{ech}^s C_{nox}^{inter}}{v_{ech}^s + k_{snox} s_{nox} \mathcal{L}_{scr} (\rho_a \theta_a)^{\beta_{snox}}} \quad (63g)$$

$$C_a^{out} = \frac{v_{ech}^s C_a^{inter} + k_{daox} \mathcal{L}_{scr} (\rho_a \theta_a)^{\beta_{daox}}}{v_{ech}^s + k_{aaox} \mathcal{L}_{scr} (\rho_a (1 - \theta_a))^{\beta_{aaox}}} \quad (63h)$$

with

$$\begin{aligned} k_{anox} &= k_{ano_2}, \quad k_{dnox} = k_{dno_2}, \quad k_{snox} = k_{sno_2}, \quad k_{inhibnox} = k_{inhibno_2}, \\ k_{rnox} &= k_{rn}, \quad k_{raox} = k_{ra}, \quad k_{rnaox} = k_{rna}, \quad k_{aaox} = k_{aa}, \quad k_{daox} = k_{da}, \quad k_{oax} = k_{oa}, \\ \beta_{anox} &= \beta_{ano_2}, \quad \beta_{dnox} = \beta_{dno_2}, \quad \beta_{snox} = \beta_{sno_2}, \\ \beta_{rnox} &= \beta_{rn}, \quad \beta_{raox} = \beta_{raox}, \quad \beta_{rnaox} = \beta_{rna}, \quad \beta_{aaox} = \beta_{aa}, \quad \beta_{daox} = \beta_{da}, \quad \beta_{oax} = \beta_{oa}, \end{aligned}$$

Proof. From (59), after a short calculation, one obtains the fully developed forms of (59d) and (59e):

$$C_{no}^{inter} = \frac{v_{ech}^n C_{no}^{in} \left(v_{ech}^n + k_{rno_2} \mathcal{L}_{pn} + \frac{k_{ano_2}}{1 + k_{inhibno_2} \theta_n} \mathcal{L}_{pn} (\rho_n (1 - \theta_n))^{\beta_{ano_2}} \right) + k_{rno_2} \mathcal{L}_{pn} \left(v_{ech}^n C_{no_2}^{in} + k_{dno_2} \mathcal{L}_{pn} (\rho_n \theta_n)^{\beta_{dno_2}} \right)}{(v_{ech}^n + k_{oxno} \mathcal{L}_{pn} + k_{ano} \mathcal{L}_{pn} (\rho_n (1 - \theta_n))^{\beta_{ano}}) \left(v_{ech}^n + k_{rno_2} \mathcal{L}_{pn} + \frac{k_{ano_2}}{1 + k_{inhibno_2} \theta_n} \mathcal{L}_{pn} (\rho_n (1 - \theta_n))^{\beta_{ano_2}} \right) - k_{rno_2} k_{oxno} \mathcal{L}_{pn}^2} \quad (65a)$$

$$C_{no_2}^{inter} = \frac{k_{oxno} \mathcal{L}_{pn} v_{ech}^n C_{no}^{in} + \left(v_{ech}^n C_{no_2}^{in} + k_{dno_2} \mathcal{L}_{pn} (\rho_n \theta_n)^{\beta_{dno_2}} \right) (v_{ech}^n + k_{oxno} \mathcal{L}_{pn} + k_{ano} \mathcal{L}_{pn} (\rho_n (1 - \theta_n))^{\beta_{ano}})}{(v_{ech}^n + k_{oxno} \mathcal{L}_{pn} + k_{ano} \mathcal{L}_{pn} (\rho_n (1 - \theta_n))^{\beta_{ano}}) \left(v_{ech}^n + k_{rno_2} \mathcal{L}_{pn} + \frac{k_{ano_2}}{1 + k_{inhibno_2} \theta_n} \mathcal{L}_{pn} (\rho_n (1 - \theta_n))^{\beta_{ano_2}} \right) - k_{rno_2} k_{oxno} \mathcal{L}_{pn}^2} \quad (65b)$$

Thus, by direct application of the assumptions of the statement, (65a) becomes :

$$C_{no}^{inter} \approx \frac{v_{ech}^n C_{no}^{in}}{k_{oxno} \mathcal{L}_{pn}} \quad (66a)$$

$$C_{no_2}^{inter} \approx \frac{v_{ech}^n C_{no}^{in} + k_{dno_2} \mathcal{L}_{pn} (\rho_n \theta_n)^{\beta_{dno_2}}}{v_{ech}^n + k_{rno_2} \mathcal{L}_{pn} + \frac{k_{ano_2}}{1 + k_{inhibno_2} \theta_n} \mathcal{L}_{pn} (\rho_n (1 - \theta_n))^{\beta_{ano_2}}} \quad (66b)$$

And then,

$$C_{no}^{inter} \approx 0 \quad (67a)$$

$$C_{no_2}^{inter} \approx \frac{v_{ech}^n C_{no}^{in} + k_{dno_2} \mathcal{L}_{pn} (\rho_n \theta_n)^{\beta_{dno_2}}}{v_{ech}^n + k_{rno_2} \mathcal{L}_{pn} + \frac{k_{ano_2}}{1 + k_{inhibno_2} \theta_n} \mathcal{L}_{pn} (\rho_n (1 - \theta_n))^{\beta_{ano_2}}} \quad (67b)$$

Recalling that $C_{no}^{in} = C_{nox}^{in}$, the resulting equations are the following :

$$C_{no}^{inter} \approx 0 \quad (68a)$$

$$C_{no_2}^{inter} \approx \frac{v_{ech}^n C_{nox}^{in} + k_{dno_2} \mathcal{L}_{pn} (\rho_n \theta_n)^{\beta_{dno_2}}}{v_{ech}^n + k_{rno_2} \mathcal{L}_{pn} + \frac{k_{ano_2}}{1 + k_{inhibno_2} \theta_n} \mathcal{L}_{pn} (\rho_n (1 - \theta_n))^{\beta_{ano_2}}} \quad (68b)$$

As a consequence of (59j)

$$C_{no}^{out} \approx 0, \quad (69)$$

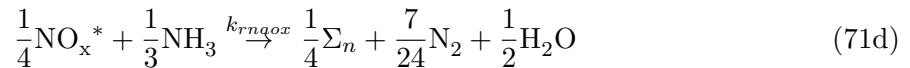
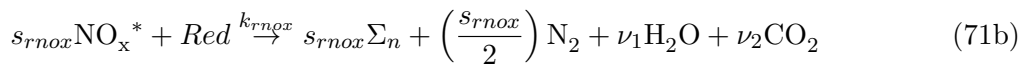
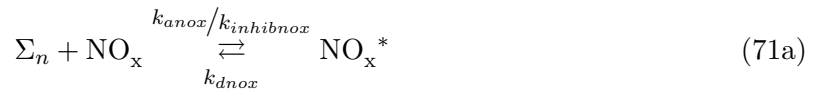
and (60) yields

$$C_{nox}^{out} \approx C_{no_2}^{out}, \quad (70)$$

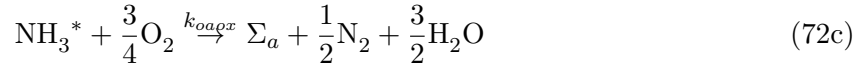
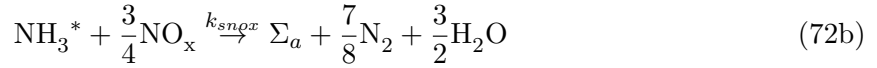
Then, considering (64) one obtains the corresponding result. This achieves the proof of Theorem 6. \square

Remark 1. One may notice that (63) is the reduced model corresponding to a LNT-SCR architecture whose chemical model is the following :

For the NO_x trap,



and for the SCR,



where $\text{NO}_x = \text{NO} + \text{NO}_2$. Theorem 6 shows that under the stated hypotheses, it is just as if all of the entering NO is immediately changed in NO_2 , which afterwards dictates the kinetics.

7 Experimental results

The tests used for calibration and validation of the models are presented in this part. The calibration of each model was carried out separately. In the case of LNT, the calibration was performed with standard driving cycles called New European Driving Cycle (NEDC). The latter is the homologation cycle for European vehicles. Validation is still to be done.

The SCR catalyst has been calibrated with stabilized driving data and then validated with another normalized cycle called Artemis cycle. The identification and validation processes are presented in the sequel.

For confidentiality reasons, the units of the quantities involved are omitted (through normalization) in the following figures.

7.1 Lean NO_x Trap catalyst

Calibration of the model has been tested with real driving tests. The challenge here is to obtain a reduced model of sufficient precision for control and monitoring.

The catalyst used has a volume of 1.9l and for these tests, NO and NO_x measurements are at disposal. As a consequence, NO_2 measurement is obtained from the equality $\text{NO}_2 = \text{NO}_x - \text{NO}$. A lambda sensor is also at disposal, which provides supplementary information about the Fuel-Air Ratio [23].

7.1.1 Method

Referring to equation (46), one can notice that the model is a highly nonlinear function of numerous parameters (30 kinetic parameters to adjust). The simultaneous identification of the kinetic parameters turns out to be complex. In order to overcome this difficulty, the reaction orders β_i are fixed according to the relative literature [12], [6]. For the other kinetic parameters, one defines a calibration vector containing the 24 model parameters to be identified (see Table 1), then, using the results of [6] as starting point one adjusts the values at best using classical optimization methods (least squares algorithm). Recall that the calibration targets are NO_x , NO and the equivalent Fuel-Air Ratio.

Parameters	ρ_n	ρ_o	k_{oxno0}	k_{rno_20}
Units	mol/m^3	mol/m^3	$(\text{mol}/\text{m}^3)^{-2} \times \text{s}^{-1}$	—
Parameters	k_{ano_20}	$k_{inhibno_20}$	k_{dno_20}	k_{ano0}
Units	$(\text{mol}/\text{m}^3)^{-2} \times \text{s}^{-1}$	$(\text{mol}/\text{m}^3)^{-2} \times \text{s}^{-1}$	$(\text{mol}/\text{m}^3)^{-2} \times \text{s}^{-1}$	$(\text{mol}/\text{m}^3)^{-2} \times \text{s}^{-1}$
Parameters	k_{rn0}	k_{ra0}	k_{rna0}	k_{ao0}
Units	$(\text{mol}/\text{m}^3)^{-2} \times \text{s}^{-1}$	$(\text{mol}/\text{m}^3)^{-2} \times \text{s}^{-1}$	$(\text{mol}/\text{m}^3)^{-2} \times \text{s}^{-1}$	$(\text{mol}/\text{m}^3)^{-2} \times \text{s}^{-1}$
Parameters	k_{rao0}	E_{oxno}	E_{rno_2}	E_{ano_2}
Units	$(\text{mol}/\text{m}^3)^{-2} \times \text{s}^{-1}$	$\text{J} \times \text{mol}^{-1}$	$\text{J} \times \text{mol}^{-1}$	$\text{J} \times \text{mol}^{-1}$
Parameters	$E_{inhibno_2}$	E_{dno_2}	E_{ano}	E_{rn}
Units	$\text{J} \times \text{mol}^{-1}$	$\text{J} \times \text{mol}^{-1}$	$\text{J} \times \text{mol}^{-1}$	$\text{J} \times \text{mol}^{-1}$
Parameters	E_{ra}	E_{rna}	E_{ao}	E_{rao}
Units	$\text{J} \times \text{mol}^{-1}$	$\text{J} \times \text{mol}^{-1}$	$\text{J} \times \text{mol}^{-1}$	$\text{J} \times \text{mol}^{-1}$

Table 1: Parameter for calibration

The real driving tests consist in the concatenation of two NEDC cycles : the first one has two rich periods and the second one is only under lean mode.

7.1.2 Results

Figure 5 and Figure 6 compare measured and calculated NO_x and NO concentrations. The model displays quite a good correlation with the experiments.

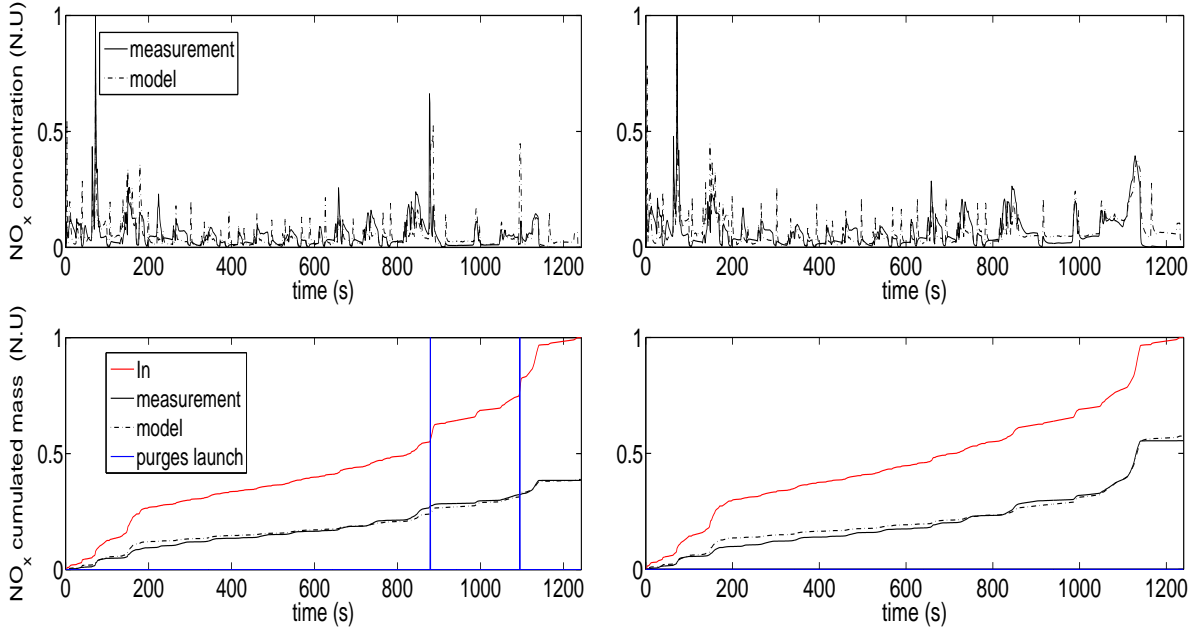


Figure 5: Comparison between experimental and simulated values of NO_x output in lean and rich conditions for NEDC experiments, the vertical lines corresponding to the beginning of the two purges.

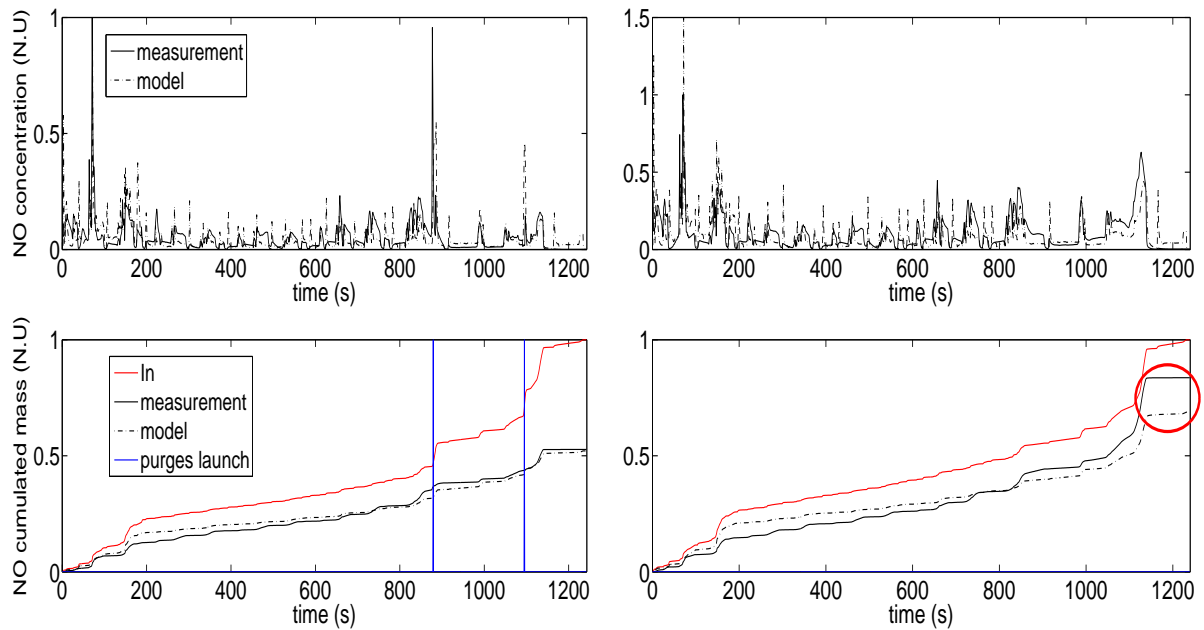


Figure 6: Comparison between experimental and simulated values of NO output in lean and rich conditions for NEDC experiments, the vertical lines corresponding to the beginning of the purges.

One can observe a deviation of the cumulated NO mass from the corresponding measurement (in the lower right corner of the lowest picture of Figure 6). This deviation may come from calibration errors on some kinetic parameters or modeling errors. It would be interesting to improve one's knowledge on the reactions implied in (9) in order to adjust the calibration results at best or propose better starting points to the optimization process.

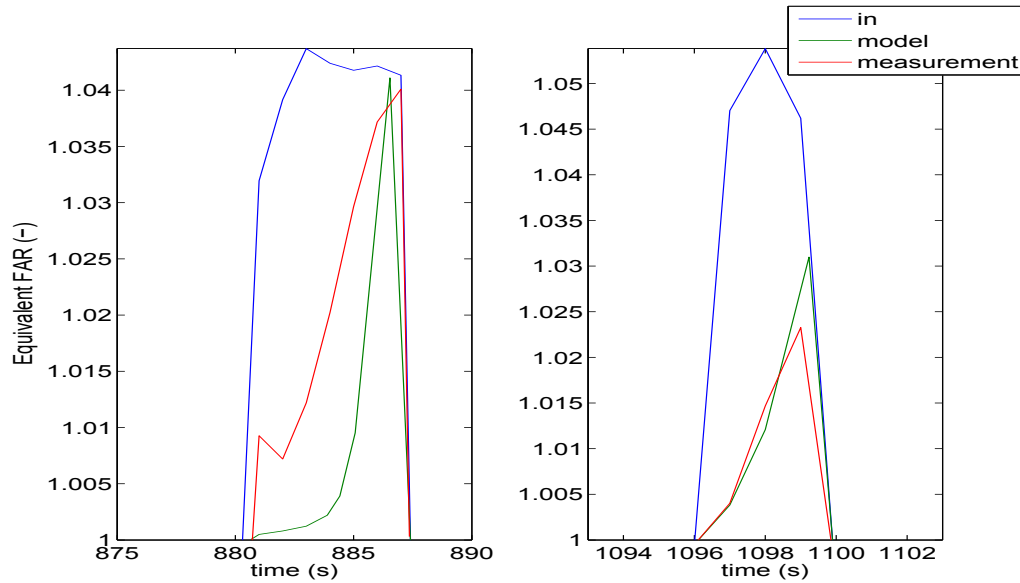


Figure 7: Comparison between experimental and simulated values of FAR. Here only the part of the part of the ratio greater than one is highlighted.

Figure 7 is a zoom in on measured and calculated value of the equivalent Fuel-Air Ratio during the purges. Representing the part of the ratio greater than one (excess of reducing species in the exhaust). It allows to identify correctly the terms of the model linked to the purges. The modeling results are less conclusive but many simplifying assumptions have been made on the regeneration process (see section 3). It would be a valuable improvement to consider each reducing species in the chemical scheme and compare the results.

7.2 SCR catalyst : Calibration

As in the previous part, the model is calibrated with real driving data. The challenge here as well is to obtain a predictive model valid on a wide range of driving conditions. The catalyst used has a volume of 2.5l. The experiment was performed with two series of data under stabilized conditions. For these tests, the calibration targets are NO_x , NO_2 and NH_3 .

7.2.1 Method

The calibration of the SCR catalyst requires less parameters than for the LNT. Therefore, one has been able to define a vector of 19 kinetic parameters to be identified (see Table 2). Similarly to the LNT calibration, the results of [24], which are the basics of this work on SCR modeling, have been taken as starting point for the optimization algorithm.

Parameters	β_{aa}	β_{da}	β_{fa}	β_{sno}
Units	—	—	—	—
Parameters	β_{sno_2}	β_{oa}	ρ_{asc}	k_{aa0}
Units	—	—	mol/m ³	(mol/m ³) ⁻² × s ⁻¹
Parameters	k_{da0}	k_{fa0}	k_{sno0}	k_{sno_20}
Units	(mol/m ³) ⁻² × s ⁻¹			
Parameters	k_{oa0}	E_{aa}	E_{da}	E_{fa}
Units	(mol/m ³) ⁻² × s ⁻¹	J × mol ⁻¹	J × mol ⁻¹	J × mol ⁻¹
Parameters	E_{sno}	E_{sno_2}	E_{oa}	
Units	J × mol ⁻¹	J × mol ⁻¹	J × mol ⁻¹	

Table 2: Parameter for calibration

7.2.2 Results

Figure 8 and Figure 9 respectively compare measured and calculated NO_x, NO₂ and NH₃ concentrations. The model displays quite a good correlation with the experiments.

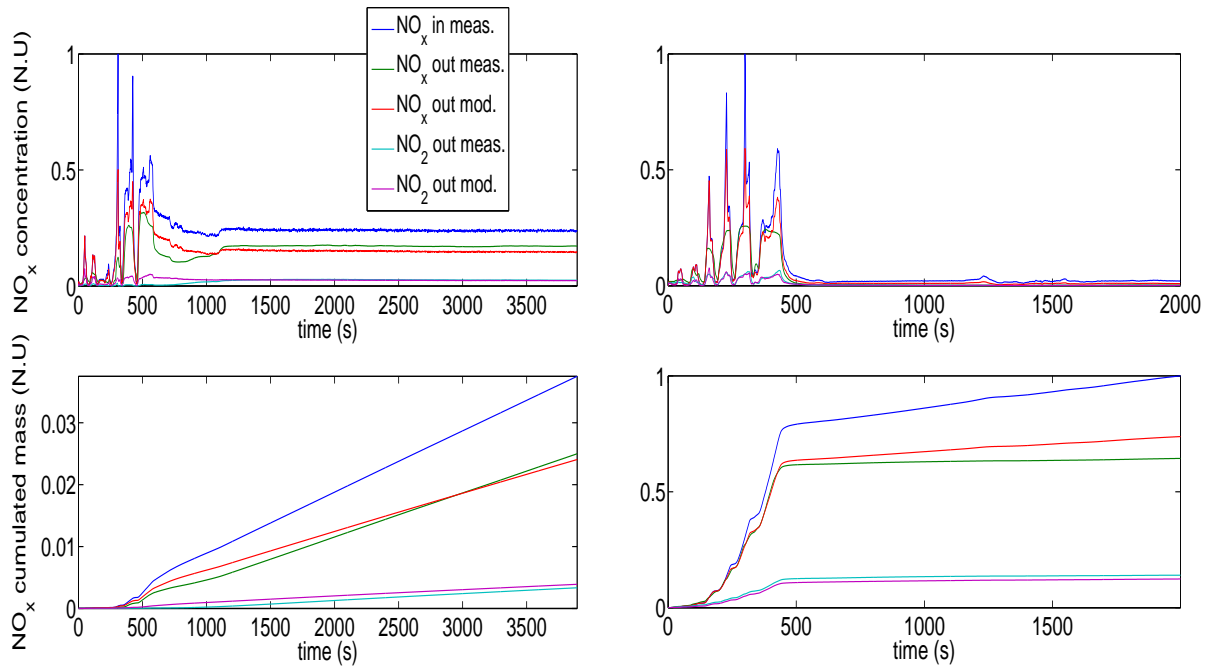


Figure 8: Comparison between experimental and simulated values of NO_x and NO₂ under the stabilized driving data.

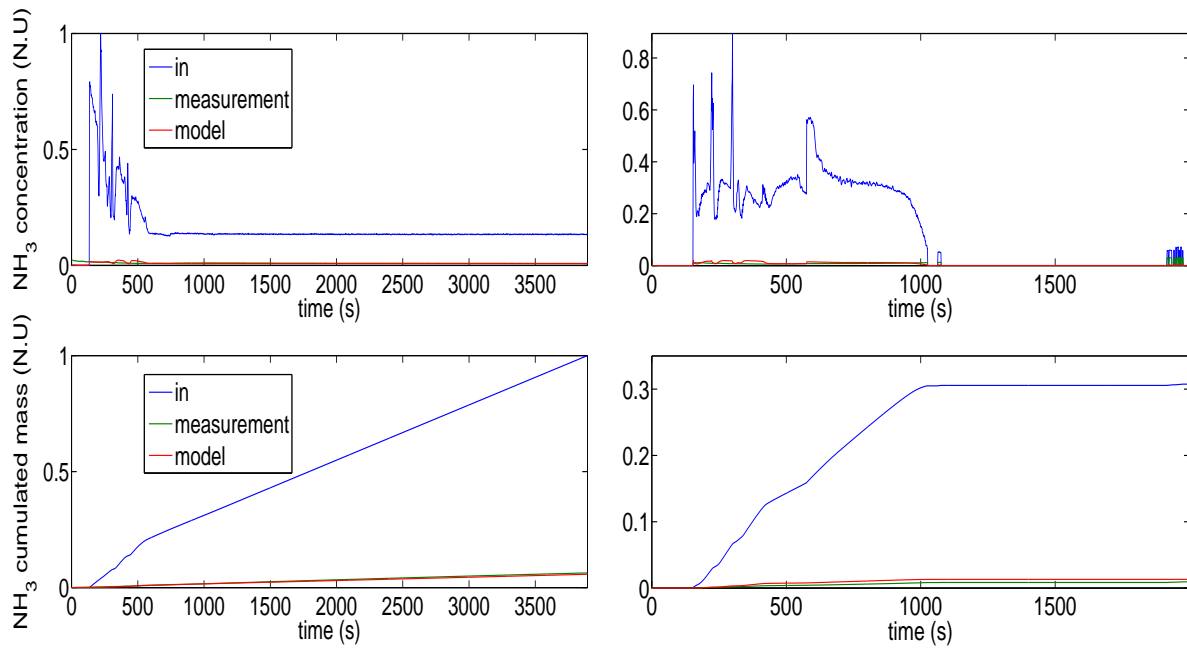


Figure 9: Comparison between experimental and simulated values of NH_3 output under the stabilized driving data.

7.3 SCR catalyst : Validation

The model has been validated afterwards, with data originating from an Artemis cycle. The catalyst used is the same (2.5l with same ageing). Such a cycle contains wider range of speed and driving modes and, as a consequence, gives better illustration of real driving conditions. Figure 10 and 11 provide the corresponding results.

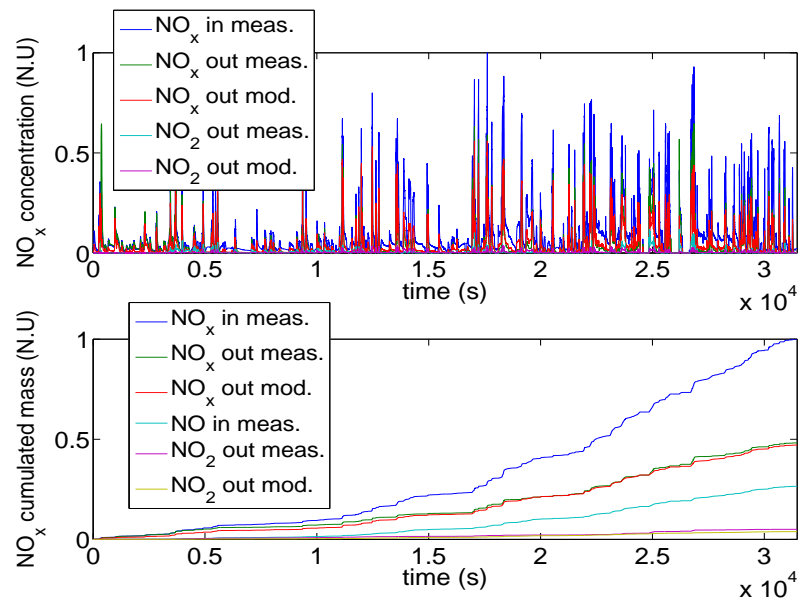


Figure 10: Comparison between experimental and simulated values of NO_x and NO_2 outputs for an Artemis experiment.

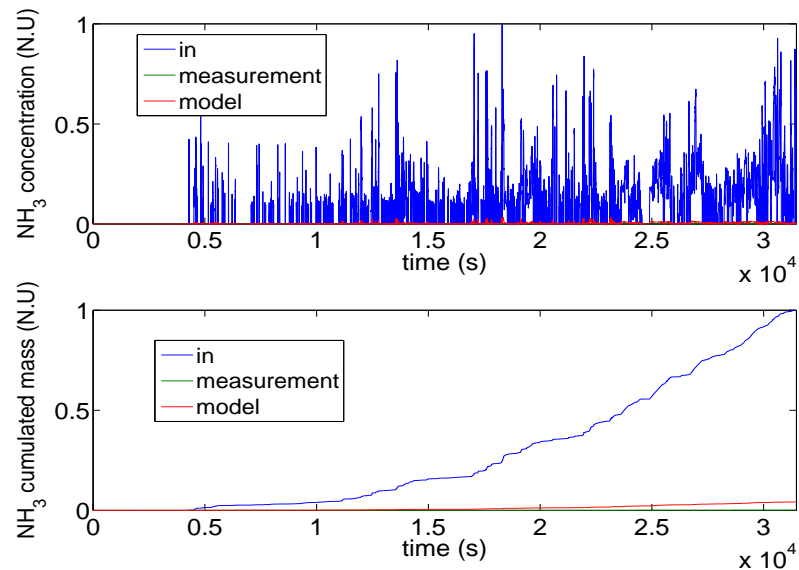


Figure 11: Comparison between experimental and simulated values of NH_3 output for an Artemis experiment.

Regarding NO and NO_2 concentration, the model fits quite well the experiment. The results for ammonia are also satisfying in spite of a deviation at the end of the cycle. One conjectures that the latter may be due to the lack of representativity during the calibration process (possibly due to the limited range of variation of temperature input).

8 Summary/Conclusions

In this paper, a step-by-step construction of reduced-order models of the LNT-SCR architecture has been performed, composed of the two models in series.

- The models have been identified separately, only calibrated for the LNT and validated as well with real driving conditions data in the case of the SCR.
- Some properties of the models have been stated and proved, permitting to estimate their accuracy.
- The models described ensure globally quite a good predictability on real driving experiments. It would be interesting to find a criterion to quantify their accuracy. This could notably permit discrimination between different architectures of after-treatment lines.
- Being built with systems of small order ODEs, the proposed models have low complexity. They will be used for future works on control and diagnosis applications.
- Lastly, some phenomena like thermal ageing of the catalysts or poisoning processes from undesirable species have not been taken into account in the model. Including these aspects in future work will lead to valuable improvement.

A Definitions/Abbreviations

A.1 Indexes/exponents

- $oxno, rno_2$: Respectively NO oxidation and NO₂ reduction,
- ano, ano_2, ao, aa : Respectively NO, NO₂, Oxygen and Ammonia adsorption,
- dno_2, da : Respectively NO₂ and Ammonia desorption,
- $inhibno_2$: Inhibition of NO₂ adsorption,
- rn, ra, rao : respectively NO_x reduction to Nitrogen , to Ammonia and Oxygen reduction,
- rna : NO_x reduction by the ammonia formed during rich period,
- oa : Ammonia oxidation,
- sno, sno_2 : Respectively NO and NO₂ reduction by stored Ammonia,
- fa : NO and NO₂ reduction by stored Ammonia ("fast reaction"),
- $in, inter, out$: Respectively LNT inlet, LNT outlet/SCR inlet, SCR outlet,

A.2 Greek/Latin letters

- v_{ech}^n, v_{ech}^s : exhaust gas speed respectively in the LNT and the SCR catalyst,
- s, ν : stoichiometric coefficients,
- $\theta_n, \theta_o, \theta_a$: Coverage fractions respectively of NO_x, Oxygen and Ammonia on the catalyst sites,
- ρ_n, ρ_o, ρ_a : Density of sites on the catalyst layer respectively for NO_x, Oxygen and Ammonia,
- T : Catalyst temperature,

- R : Gas constant,
- $\mathcal{L}_{pn}, \mathcal{L}_{scr}$: Length respectively of the LNT and the SCR catalysts.

B Proof of (45)

$$p_2 p_1 - p_3 = -j_{b11} j_{b22} (j_{b11} + j_{b22}) + j_{b14} j_{b41} (j_{b11} + 2j_{b22} + j_{b44}) + j_{b24} j_{b42} (j_{b22} + 2j_{b11} + j_{b44}) - (j_{b11} + j_{b22} + j_{b44}) j_{b44} (j_{b11} + j_{b22})$$

Observing that :

$$j_{b44} = \frac{1}{\rho_o} (-j_{b14} + j_{b24}) \quad (73a)$$

$$j_{b11} = -\frac{v_{ech}^n}{\mathcal{L}_{pn}} - j_{b41} \rho_o \quad (73b)$$

$$j_{b22} = -\frac{v_{ech}^n}{\mathcal{L}_{pn}} - \mathcal{X}(\theta_n) + j_{b42} \rho_o, \text{ where } \mathcal{X}(\theta_n) \text{ is defined in (35)} \quad (73c)$$

we then obtain :

$$\begin{aligned} p_2 p_1 - p_3 &= -j_{b11} j_{b22} (j_{b11} + j_{b22}) \\ &+ j_{b14} j_{b41} \left[-3 \frac{v_{ech}^n}{\mathcal{L}_{pn}} - 2\mathcal{X}(\theta_n) + \frac{1}{\rho_o} (j_{b24} - j_{b14}) + \rho_o (2j_{b42} - j_{b41}) \right] \\ &+ j_{b24} j_{b42} \left[-3 \frac{v_{ech}^n}{\mathcal{L}_{pn}} - \mathcal{X}(\theta_n) + \frac{1}{\rho_o} (j_{b24} - j_{b14}) + \rho_o (j_{b42} - 2j_{b41}) \right] \\ &- \frac{1}{\rho_o} (j_{b24} - j_{b14}) \left[-2 \frac{v_{ech}^n}{\mathcal{L}_{pn}} - \mathcal{X}(\theta_n) + \rho_o (j_{b42} - j_{b41}) \right] \left[-2 \frac{v_{ech}^n}{\mathcal{L}_{pn}} - \mathcal{X}(\theta_n) + \frac{1}{\rho_o} (j_{b24} - j_{b14}) + \rho_o (j_{b42} - j_{b41}) \right] \\ &= -j_{b11} j_{b22} (j_{b11} + j_{b22}) \\ &+ j_{b14} j_{b41} \left[-2 \frac{v_{ech}^n}{\mathcal{L}_{pn}} - \mathcal{X}(\theta_n) + \frac{1}{\rho_o} (j_{b24} - j_{b14}) + \rho_o (j_{b42} - j_{b41}) \right] + j_{b14} j_{b41} \left(-\frac{v_{ech}^n}{\mathcal{L}_{pn}} - \mathcal{X}(\theta_n) + \rho_o j_{b42} \right) \\ &+ j_{b24} j_{b42} \left[-2 \frac{v_{ech}^n}{\mathcal{L}_{pn}} - \mathcal{X}(\theta_n) + \frac{1}{\rho_o} (j_{b24} - j_{b14}) + \rho_o (j_{b42} - j_{b41}) \right] + j_{b24} j_{b42} \left(-\frac{v_{ech}^n}{\mathcal{L}_{pn}} - \rho_o j_{b41} \right) \\ &+ \left[\left(2 \frac{v_{ech}^n}{\mathcal{L}_{pn}} + \mathcal{X}(\theta_n) \right) \frac{1}{\rho_o} (j_{b24} - j_{b14}) - j_{b24} j_{b42} + j_{b24} j_{b41} + j_{b14} j_{b42} - j_{b14} j_{b41} \right] \times \\ &\quad \times \left[-2 \frac{v_{ech}^n}{\mathcal{L}_{pn}} - \mathcal{X}(\theta_n) + \frac{1}{\rho_o} (j_{b24} - j_{b14}) + \rho_o (j_{b42} - j_{b41}) \right] \end{aligned}$$

A first simplification gives :

$$\begin{aligned} p_2 p_1 - p_3 &= -j_{b11} j_{b22} (j_{b11} + j_{b22}) + j_{b14} j_{b41} \left(-\frac{v_{ech}^n}{\mathcal{L}_{pn}} - \mathcal{X}(\theta_n) + \rho_o j_{b42} \right) + j_{b24} j_{b42} \left(-\frac{v_{ech}^n}{\mathcal{L}_{pn}} - \rho_o j_{b41} \right) \\ &+ \left[\left(2 \frac{v_{ech}^n}{\mathcal{L}_{pn}} + \mathcal{X}(\theta_n) \right) \frac{1}{\rho_o} (j_{b24} - j_{b14}) + j_{b24} j_{b41} + j_{b14} j_{b42} \right] \left[-2 \frac{v_{ech}^n}{\mathcal{L}_{pn}} - \mathcal{X}(\theta_n) + \frac{1}{\rho_o} (j_{b24} - j_{b14}) + \rho_o (j_{b42} - j_{b41}) \right] \end{aligned}$$

then, developing the fourth term of the previous expression gives :

$$\begin{aligned}
 p_2 p_1 - p_3 &= -j_{b11} j_{b22} (j_{b11} + j_{b22}) + j_{b14} j_{b41} \left(-\frac{v_{ech}^n}{\mathcal{L}_{pn}} - \mathcal{X}(\theta_n) + \rho_o j_{b42} \right) + j_{b24} j_{b42} \left(-\frac{v_{ech}^n}{\mathcal{L}_{pn}} - \rho_o j_{b41} \right) \\
 &+ \left(2 \frac{v_{ech}^n}{\mathcal{L}_{pn}} + \mathcal{X}(\theta_n) \right) \frac{1}{\rho_o} (j_{b24} - j_{b14}) \left[-2 \frac{v_{ech}^n}{\mathcal{L}_{pn}} - \mathcal{X}(\theta_n) + \frac{1}{\rho_o} (j_{b24} - j_{b14}) + \rho_o (j_{b42} - j_{b41}) \right] \\
 &+ j_{b24} j_{b41} \left[-2 \frac{v_{ech}^n}{\mathcal{L}_{pn}} - \mathcal{X}(\theta_n) + \frac{1}{\rho_o} (j_{b24} - j_{b14}) + \rho_o (j_{b42} - j_{b41}) \right] \\
 &+ j_{b14} j_{b42} \left[-2 \frac{v_{ech}^n}{\mathcal{L}_{pn}} - \mathcal{X}(\theta_n) + \frac{1}{\rho_o} (j_{b24} - j_{b14}) + \rho_o (j_{b42} - j_{b41}) \right]
 \end{aligned}$$

We rewrite the previous expression under the form (notice the change in the second line) :

$$\begin{aligned}
 p_2 p_1 - p_3 &= -j_{b11} j_{b22} (j_{b11} + j_{b22}) + j_{b14} j_{b41} \left(-\frac{v_{ech}^n}{\mathcal{L}_{pn}} - \mathcal{X}(\theta_n) + \rho_o j_{b42} \right) + j_{b24} j_{b42} \left(-\frac{v_{ech}^n}{\mathcal{L}_{pn}} - \rho_o j_{b41} \right) \\
 &+ \left(\frac{v_{ech}^n}{\mathcal{L}_{pn}} + \mathcal{X}(\theta_n) + \frac{v_{ech}^n}{\mathcal{L}_{pn}} \right) \frac{1}{\rho_o} (j_{b24} - j_{b14}) \left[-2 \frac{v_{ech}^n}{\mathcal{L}_{pn}} - \mathcal{X}(\theta_n) + \frac{1}{\rho_o} (j_{b24} - j_{b14}) + \rho_o (j_{b42} - j_{b41}) \right] \\
 &+ j_{b24} j_{b41} \left[-2 \frac{v_{ech}^n}{\mathcal{L}_{pn}} - \mathcal{X}(\theta_n) + \frac{1}{\rho_o} (j_{b24} - j_{b14}) + \rho_o (j_{b42} - j_{b41}) \right] \\
 &+ j_{b14} j_{b42} \left[-2 \frac{v_{ech}^n}{\mathcal{L}_{pn}} - \mathcal{X}(\theta_n) + \frac{1}{\rho_o} (j_{b24} - j_{b14}) + \rho_o (j_{b42} - j_{b41}) \right]
 \end{aligned}$$

and further developments lead to :

$$\begin{aligned}
 p_2 p_1 - p_3 &= -j_{b11} j_{b22} (j_{b11} + j_{b22}) + j_{b14} j_{b41} \left(-\frac{v_{ech}^n}{\mathcal{L}_{pn}} - \mathcal{X}(\theta_n) + \rho_o j_{b42} \right) + j_{b24} j_{b42} \left(-\frac{v_{ech}^n}{\mathcal{L}_{pn}} - \rho_o j_{b41} \right) \\
 &+ \left(\frac{v_{ech}^n}{\mathcal{L}_{pn}} + \mathcal{X}(\theta_n) \right) \frac{1}{\rho_o} j_{b24} \left[-2 \frac{v_{ech}^n}{\mathcal{L}_{pn}} - \mathcal{X}(\theta_n) + \frac{1}{\rho_o} (j_{b24} - j_{b14}) + \rho_o (j_{b42} - j_{b41}) \right] + \frac{v_{ech}^n}{\mathcal{L}_{pn}} j_{b24} j_{b42} \\
 &+ \frac{v_{ech}^n}{\mathcal{L}_{pn}} \frac{1}{\rho_o} j_{b24} \left[-2 \frac{v_{ech}^n}{\mathcal{L}_{pn}} - \mathcal{X}(\theta_n) + \frac{1}{\rho_o} (j_{b24} - j_{b14}) - \rho_o j_{b41} \right] \\
 &+ \left(\frac{v_{ech}^n}{\mathcal{L}_{pn}} + \mathcal{X}(\theta_n) \right) j_{b14} j_{b41} + \left(\frac{v_{ech}^n}{\mathcal{L}_{pn}} + \mathcal{X}(\theta_n) \right) \frac{1}{\rho_o} j_{b14} \left[-2 \frac{v_{ech}^n}{\mathcal{L}_{pn}} - \mathcal{X}(\theta_n) + \frac{1}{\rho_o} (j_{b24} - j_{b14}) + \rho_o j_{b42} \right] \\
 &- \frac{v_{ech}^n}{\mathcal{L}_{pn}} \frac{1}{\rho_o} j_{b14} \left[-2 \frac{v_{ech}^n}{\mathcal{L}_{pn}} - \mathcal{X}(\theta_n) + \frac{1}{\rho_o} (j_{b24} - j_{b14}) + \rho_o (j_{b42} - j_{b41}) \right] \\
 &+ j_{b24} j_{b41} \rho_o j_{b42} + j_{b24} j_{b41} \left[-2 \frac{v_{ech}^n}{\mathcal{L}_{pn}} - \mathcal{X}(\theta_n) + \frac{1}{\rho_o} (j_{b24} - j_{b14}) - \rho_o j_{b41} \right] \\
 &- j_{b14} j_{b42} \rho_o j_{b41} + j_{b14} j_{b42} \left[-2 \frac{v_{ech}^n}{\mathcal{L}_{pn}} - \mathcal{X}(\theta_n) + \frac{1}{\rho_o} (j_{b24} - j_{b14}) + \rho_o j_{b42} \right]
 \end{aligned}$$

Putting together the last term of 2nd line and 5th line, and the first term of 4th line with the

first term of last line, one factorizes this expression in the following manner :

$$\begin{aligned}
p_2 p_1 - p_3 = & -j_{b11} j_{b22} (j_{b11} + j_{b22}) + j_{b14} j_{b41} \left(-\frac{v_{ech}^n}{\mathcal{L}_{pn}} - \mathcal{X}(\theta_n) + \rho_o j_{b42} \right) + j_{b24} j_{b42} \left(-\frac{v_{ech}^n}{\mathcal{L}_{pn}} - \rho_o j_{b41} \right) \\
& + \left(\frac{v_{ech}^n}{\mathcal{L}_{pn}} + \mathcal{X}(\theta_n) \right) \frac{1}{\rho_o} j_{b24} \left[-2 \frac{v_{ech}^n}{\mathcal{L}_{pn}} - \mathcal{X}(\theta_n) + \frac{1}{\rho_o} (j_{b24} - j_{b14}) + \rho_o (j_{b42} - j_{b41}) \right] \\
& + \frac{v_{ech}^n}{\mathcal{L}_{pn}} \frac{1}{\rho_o} j_{b24} \left[-2 \frac{v_{ech}^n}{\mathcal{L}_{pn}} - \mathcal{X}(\theta_n) + \frac{1}{\rho_o} (j_{b24} - j_{b14}) - \rho_o j_{b41} \right] \\
& + \left(\frac{v_{ech}^n}{\mathcal{L}_{pn}} + \mathcal{X}(\theta_n) \right) \frac{1}{\rho_o} j_{b14} \left[-2 \frac{v_{ech}^n}{\mathcal{L}_{pn}} - \mathcal{X}(\theta_n) + \frac{1}{\rho_o} (j_{b24} - j_{b14}) + \rho_o j_{b42} \right] \\
& - \frac{v_{ech}^n}{\mathcal{L}_{pn}} \frac{1}{\rho_o} j_{b14} \left[-2 \frac{v_{ech}^n}{\mathcal{L}_{pn}} - \mathcal{X}(\theta_n) + \frac{1}{\rho_o} (j_{b24} - j_{b14}) + \rho_o (j_{b42} - j_{b41}) \right] \\
& + j_{b24} j_{b41} \left[-2 \frac{v_{ech}^n}{\mathcal{L}_{pn}} - \mathcal{X}(\theta_n) + \frac{1}{\rho_o} (j_{b24} - j_{b14}) - \rho_o j_{b41} \right] \\
& + j_{b14} j_{b42} \left[-2 \frac{v_{ech}^n}{\mathcal{L}_{pn}} - \mathcal{X}(\theta_n) + \frac{1}{\rho_o} (j_{b24} - j_{b14}) + \rho_o j_{b42} \right] \\
& + j_{b14} j_{b41} \left(\frac{v_{ech}^n}{\mathcal{L}_{pn}} + \mathcal{X}(\theta_n) - \rho_o j_{b42} \right) + j_{b24} j_{b42} \left(\frac{v_{ech}^n}{\mathcal{L}_{pn}} + \rho_o j_{b41} \right)
\end{aligned}$$

Then, after two simplifications of the terms from first and last lines and a further factorization we obtain :

$$\begin{aligned}
p_2 p_1 - p_3 = & -j_{b11} j_{b22} (j_{b11} + j_{b22}) \\
& + \left[j_{b14} j_{b42} - j_{b14} \frac{1}{\rho_o} \left(\frac{v_{ech}^n}{\mathcal{L}_{pn}} + \mathcal{X}(\theta_n) \right) \right] \left[-2 \frac{v_{ech}^n}{\mathcal{L}_{pn}} - \mathcal{X}(\theta_n) + \frac{1}{\rho_o} (j_{b24} - j_{b14}) + \rho_o j_{b42} \right] \\
& + \left[j_{b24} j_{b41} + j_{b24} \frac{1}{\rho_o} \frac{v_{ech}^n}{\mathcal{L}_{pn}} \right] \left[-2 \frac{v_{ech}^n}{\mathcal{L}_{pn}} - \mathcal{X}(\theta_n) + \frac{1}{\rho_o} (j_{b24} - j_{b14}) - \rho_o j_{b41} \right] \\
& + \left[-j_{b14} \frac{1}{\rho_o} \frac{v_{ech}^n}{\mathcal{L}_{pn}} + j_{b24} \frac{1}{\rho_o} \left(\frac{v_{ech}^n}{\mathcal{L}_{pn}} + \mathcal{X}(\theta_n) \right) \right] \left[-2 \frac{v_{ech}^n}{\mathcal{L}_{pn}} - \mathcal{X}(\theta_n) + \frac{1}{\rho_o} (j_{b24} - j_{b14}) + \rho_o (j_{b42} - j_{b41}) \right]
\end{aligned}$$

Finally, with the help of (73a), we obtain :

$$\begin{aligned}
p_2 p_1 - p_3 = & -j_{b11} j_{b22} (j_{b11} + j_{b22}) \\
& + j_{b14} \left(j_{b42} - \frac{1}{\rho_o} \left(\frac{v_{ech}^n}{\mathcal{L}_{pn}} + \mathcal{X}(\theta_n) \right) \right) \left(-2 \frac{v_{ech}^n}{\mathcal{L}_{pn}} - \mathcal{X}(\theta_n) + j_{b42} \rho_o + j_{b44} \right) \\
& + j_{b24} \left(j_{b41} + \frac{1}{\rho_o} \frac{v_{ech}^n}{\mathcal{L}_{pn}} \right) \left(-2 \frac{v_{ech}^n}{\mathcal{L}_{pn}} - \mathcal{X}(\theta_n) - j_{b41} \rho_o + j_{b44} \right) \\
& + \left(j_{b44} \frac{v_{ech}^n}{\mathcal{L}_{pn}} + j_{b24} \frac{\mathcal{X}(\theta_n)}{\rho_o} \right) (j_{b11} + j_{b22} + j_{b44})
\end{aligned}$$

This achieves the proof of (45).

References

- [1] R. Snow, G. Cavatatio, D. Dobson, C. Montreuil, and R. Hammerle. Calibration of a LNT-SCR Diesel Aftertreatment System. *SAE Technical Paper Series*, April 2007. 2007-28-1244.
- [2] J. Theis and E. Gulari. A LNT+SCR System for Treating the NO_x Emissions from a Diesel Engine. *SAE Technical Paper*, 2006. 2006-01-0219.
- [3] J. Parks and V. Prikhodko. Ammonia Production and Utilization in Hybrid LNT+SCR System. *SAE Technical Paper*, 2009. 2009-01-2739.
- [4] D. Chatterjee, P. Koci, V. Schmeisser, and M. Marek. Modelling of NO_x storage + SCR Exhaust Gas Aftertreatment System with Internal Generation of Ammonia. *SAE Int. J. Fuels Lubr*, pages 500–522, 2010. 2010-01-0887.
- [5] D. Marie-Luce, P-A Bliman, D. Di-Penta, and M. Sorine. Control Oriented Modeling of a LNT-SCR After-Treatment Architecture. *SAE International Journal of Engines*, pages 1764–1775, June 2011. 2011-01-1307.
- [6] A. Lindholm, N.W. Currier, J. Li, A. Yezerets, and L. Olsson. Detailed kinetic modeling of NO_x storage and reduction with hydrogen as the reducing agent and in the presence of CO₂ and H₂O over a Pt–Ba/Al catalyst. *Journal of catalysis*, July 2008.
- [7] L.Lietti, I. Nova, and P. Forzatti. Role of Ammonia in the Reduction by Hydrogen of NO_x Stored over Pt–Ba/Al₂O₃ Lean NO_x Trap Catalyst. *Journal of catalysis*, June 2008.
- [8] L.Lietti, I. Nova, and P. Forzatti. Mechanistic Aspects of the Reduction of Stored NO_x over Pt–Ba/Al₂O₃ Lean NO_x Trap Systems. *Catalysis Today*, March 2008.
- [9] M. Schaefer, L. Hofmann, P. Giroto, and R. Rohe. Investigation of NO_x-and PM-reduction by a Combination of SCR-catalyst and Diesel Particulate Filter for Heavy-Duty Diesel Engine. *SAE Int. J. Fuels Lubr*, pages 386–398, 2009. 2009-01-0912.
- [10] A.P.E. York, M. Ahmadinejad, T.C. Watling, and A.P. Walker. Modeling of the Catalized Continuously Regenerated Diesel Particulate Filter (CCR-DPF) System : Model Development and Passive Regeneration Studies. *SAE Technical Paper*, 2007. 2007-01-0043.
- [11] L. Cao, J.L. Ratts, A. Yezerets, N.W. Currier, J.M. Caruthers, W.N. Delgass, and F.H. Ribeiro. Kinetic Modeling of NO_x Storage/Reduction on Pt–Ba/Al₂O₃ Monolith Catalysts. *Industrial & Engineering Chemistry*, July 2008.
- [12] M. Sharma, K. Kabin, M.P. Harold, and V. Balakotaiah. Modeling of NO_x storage and reduction for Diesel Exhaust Emission Control. *SAE Technical Paper Series*, April 2005. 2005-01-0972.
- [13] A. Manigrasso, P. Darcy, and P. Da Costa. Modeling of a Lean NO_x Trap System with NO/NO₂ Differentiation. *SAE INT. J. Fuels Lubr.*, pages 414–424, 2010. 2010-01-1554.
- [14] M. Milh and H. Westberg. Reduction of NO₂ Stored in a Commercial Lean NO_x Trap at Low Temperatures. *Topics in catalysis*, May 2007.
- [15] J. Parks, S. Huff, J. Pihl, and J.S. Choi. Nitrogen Selectivity in Lean NO_x Trap Catalysis with Diesel Engine In-Cylinder Regeneration. *SAE Technical Paper*, 2005. 2005-01-3876.

- [16] D. Terribile, J. Llorca, M. Boaro, C. de Leitenburg, G. Dolcetti, and A. Trovarelli. Fast Oxygen Uptakes/Release over a New CeO_x Phase. *Chemical Communications*, 17:1897–1898, 1998.
- [17] J.C. Wurzenberg and R. Wanker. Multi-Scale SCR Modeling, 1D Kinetic Analysis and 3D System Simulation. *SAE Technical paper series*, April 2005. 2005-01-0948.
- [18] C.M. Schär, C.H. Onder, H.P. Geering, and M. Elsener. Control of a Urea SCR Catalytic Converter System for a Mobile Heavy Duty Diesel Engine. *SAE Technical Paper Series*, March 2003. 2003-01-0776.
- [19] Q. Song and G. Zhu. Model-based Close-loop Control of Urea SCR Exhaust Aftertreatment System for Diesel Engine. *SAE Technical Paper Series*, March 2002. 2002-01-0287.
- [20] I. Nova, C. Ciardelli, E. Tronconi, D.I. Chatterjee, and M. Weibel. NH_3 – NO/NO_2 SCR for Diesel Exhausts After Treatment : Mechanism and Modelling of a Catalytic Converter. *Topics in catalysis*, 2007.
- [21] P. Kokotović, H. Khalil, and J. O’Reily. *Singular Perturbation in Control : Analysis and Design*. SIAM, 1999.
- [22] A. N. Tikhonov. Systems of differential equations containing small parameters multiplying the derivatives. *Mat. Sborn.*, 31:575–586, 1952.
- [23] W. Chatlatanagulchai, K. Yaovaja, S. Rhienprayoon, and K. Wannatong. Air-Fuel Ratio Regulation with Optimum Throttle Opening in Diesel-Dual-Fuel Engine. *SAE Technical Paper*, 2010. 2010-01-1574.
- [24] A. Joshi, Y. Jiang, P. Flörchinger, and S. Ogunwumi. Two-dimensional transient monolith model for selective catalytic reduction using vanadia-based catalyst. *SAE technical paper series*, 2008. 2008-28-0022.
- [25] C. Enderle, G. Vent, and M. Paule. Bluetec Diesel Technology - Clean, Efficient and Powerful. *SAE Technical Paper*, 2008. 2008-01-1182.
- [26] S. Hackenberg and M. Ranalli. Ammonia on a LNT : Avoid the Formation or Take Advantage of It. *SAE Technical Paper*, 2007. 2007-01-1239.
- [27] A. Ketfi-Cherif, D. Von Wissel, S. Beurthey, and M. Sorine. Modeling and Control of a NO_x Trap catalyst. *SAE Technical Paper*, 2000. 2000-01-1199.
- [28] J.R. Theis, J.A. Ura, and R.W. McCabe. The Effects of Sulfur Poisoning and Desulfatation Temperature on the NO_x Conversion of LNT+SCR Systems for Diesel Applications. *SAE Int. J. Fuels Lubr.*, pages 1–15, 2010. 2010-01-0300.
- [29] L. Hofmann, K. Rusch, S. Fischer, and B. Lemire. Onboard Emissions Monitoring on a HD Truck with an SCR System Using NO_x Sensors. *SAE Technical Paper Series*, March 2004. 2004-01-1290.
- [30] W. S. Epling, L. E. Campbell, A. Yezerets, N. W. Currier, and J. E. Parks. Overview of the Fundamental Reactions and Degradation Mechanisms of NO_x Storage/Reduction Catalysts. *Catalysis Reviews. Science and engineering*, 46(2):163–245, 2004.

-
- [31] A. Schuler, M. Votsmeier, P. Kiwic, J. Gieshoff, W. Hauptmann, A. Drochner, and H. Vogel. NH₃-SCR on Fe zeolite catalysts - From model setup to NH₃ dosing. *Chemical Engineering Journal*, pages 333–340, 2009.
- [32] P. Forzatti, L. Castoldi, L. Lietti, I. Nova, and E. Tronconi. Identification of the Reaction Networks of the NO_x Storage:Reduction in Lean NO_x Trap Systems. *Elsevier*, 2007.
- [33] N. Kato, K. Nakagaki, and N. Ina. Thick Film ZrO₂ NO_x Sensor. *SAE Technical Paper Series*, February 1996. 960334.
- [34] N. Kato, H. Kurachi, and Y. Hamada. Thick Film ZrO₂ NO_x Sensor for the Measurement of Low NO_x Concentration. *SAE Technical Paper Series*, February 1998. 980170.
- [35] J. Kim, J. Sun, I. Kolmanovsky, and J. Koncsol. A Phenomenological Control Oriented Lean NO_x Trap Model. *Proc SAE World Congress*, 2003.
- [36] L. Cummaranatunge, S.S. Mulla, A. Yezerets, N.W. Currier, W.N. Delgass, and F.H. Ribeiro. Ammonia is a Hydrogen Carrier in the Regeneration of Pt/BaO/Al₂O₃ NO_x Trap with H₂. *Journal of catalysis*, December 2006.
- [37] L. Olsson and B. Andersson. Kinetic modeling in automotive catalysis. *Topics in catalysis*, april 2004.
- [38] J. H. Bik, S. D. Yim, I-S Nam, J-H Lee, B.K. Cho, and S.H. Oh. Control of NO_x emissions from Diesel engine by selective catalytic reduction (SCR) with urea. *Topics in catalysis*, 2004.



**RESEARCH CENTRE
PARIS – ROCQUENCOURT**

Domaine de Voluceau, - Rocquencourt
B.P. 105 - 78153 Le Chesnay Cedex

Publisher
Inria
Domaine de Voluceau - Rocquencourt
BP 105 - 78153 Le Chesnay Cedex
inria.fr

ISSN 0249-6399